2010

Development of fluorescence-based methods for non-invasive measurement of integrin microclustering

Deepak Dibya
Iowa State University

Development of fluorescence-based methods for non-invasive measurement of integrin microclustering

by

Deepak Dibya

A dissertation submitted to the graduate faculty

in partial fulfillment of the requirements for the degree of

DOCTOR OF PHILOSOPHY

Major: Analytical Chemistry

Program of Study Committee:
Emily A. Smith, Major Professor
Robert S. Houk
Victor Shang-Yi Lin
Klaus Schmidt-Rohr
Balaji Narasimhan

Iowa State University

Ames, Iowa

2010

To my Families and Friends

TABLE OF CONTENTS

ACKNOWLEDGEMENTS v

CHAPTER 1: General Introduction

1. Dissertation Motivation and Overview 1
2. Literature Review 4
3. Dissertation Organization 19
4. References 20

CHAPTER 2: Identifying cytoplasmic proteins that affect receptor clustering using fluorescence resonance energy transfer and RNA interference

1. Abstract 27
2. Introduction 28
3. Experimental 31
4. Results and Discussion 35
5. Conclusion 44
6. Acknowledgements 45
7. References 45

CHAPTER 3: Non-invasive Measurements of Cholesterol's Role in Integrin Microclustering

1. Abstract 59
2. Introduction 60
3. Materials and Methods 62
4. Results and Discussion 67
5. Conclusion 74
6. Acknowledgements 75
7. References 75

CHAPTER 4: Conclusions

1. General Conclusions 93
2. Future Prospects 94
3. References 95

APPENDIX I: Statistical Analysis of FRET and FRAP data 96

APPENDIX II: Expression, Purification and Estimation of Taq DNA Polymerase 101

APPENDIX III: Synthesis of double stranded RNA 106

VITA 111

Acknowledgments

I am deeply thankful to many people in my life for all my accomplishments. I will start with my parents, Mr. Jagdish Prasad Gupta and Vinita Devi, my siblings Poonam di, Arun and Anup for all the love, care and support they have given me. I would also like to thank my brother Santosh Gupta and brother-in law Raju Gupta for being a role model for me and Arjun chacha, for showing me the importance of hard work early on in my life.

It is difficult to overstate my gratitude to my Ph. D. supervisor, Prof. Emily Smith, for warmly welcoming me in the group and introducing me to the wonderful research areas. I thank her for elegantly handling all the aspects of graduation including my dissertation composition. I thank her for being approachable and not to mention the lengthy discussions on different projects that have made me a better scientist. In addition, I thank her for providing me the opportunity to supervise several students within research laboratory. The opportunities provided in Smith group trained me in all the aspects of graduate career such as designing and conducting experiments, collecting, analyzing and interpreting the data, presenting scientific results in regional and national meetings, writing manuscripts and technical reports for funding agencies. Emily, you provide a learning and congenial atmosphere in the lab that gave me freedom to do research in my own way, especially the cholesterol project, making me more independent. Your constant encouragement and support guided me well throughout the graduate school career. Thank you for all this.

My first three years in graduate school with Prof. Marc Porter was a fairly steep learning slope for me. I truly thank Prof. Porter for being encouraging and an excellent educator in imparting the true essence of quality.

I thank Prof. Yeung for being very patient with my plethora of questions that I asked him during the coursework. I thank his efforts in explaining complex concepts in a lucid and simple manner and teaching me the idea that a simple solution is always the best solution. Your guidance made analytical chemistry fun for me.

Thanks Bob Lipert for always having time to talk with me and teaching me the important concepts and problem solving skills that one would require during research.

I would like to thank my schoolteacher Dr. A. K. Sharma for making me good at mathematics and Ms. Raman for teaching me chemistry to a point that encouraged me for higher studies.

Thank you dear friends: Eklavya, Sachet Shukla, Abhishek Bandopadhya, Ravindra Singh, Ravi Jha, Sandeep Diwakar, Ashish Kapahi and Kundan Kumar, for all your camaraderie.

I would also like to thank all the Smith group members and past Porter group members: Suzanne, Neha, Cherry, Kris, Jason, Matt, Jeremy, Betsy, John, Rachel, Gaby, Dave, April, Nikola, Sebastian Gufeng for their insightful comments during practice talks, group meetings and the manuscript editing. Special thanks to Neha for her great help during the last stretch of graduate studies.

My wife, I cannot thank you enough. Without you it wouldn't have been possible.

CHAPTER 1: General Introduction

DISSERTATION MOTIVATION AND OVERVIEW

A deeper understanding of the cell membrane organization can ultimately lead to a new or improved therapeutics target. For example, the majority of the drugs for various ailments are targeted towards the cell membrane and its components. A class of membrane proteins called receptors transmits signals across the cell membrane and is considered fundamental to the functioning of an organism. Abnormality in transmitting signals during cell signaling events can lead to a variety of pathological conditions. A class of receptors called integrins is vital for many cellular processes that include adhesion, motility, growth and survival. Microclustering of integrins have been shown to mediate many cell signaling processes. Aberrant integrin mediated cell signaling has been implicated in various cancer metastases. Current methods are capable of measuring integrin microclustering but have not been utilized in relating the cellular components that affects the integrin microclustering.

In order to better understand the cell signaling process, non-invasive methods to measure the integrin microclustering and examine the factors affecting the dynamics of these clusters are needed. This dissertation is focused on the development of non-invasive analytical tools to investigate the role of cytoplasmic proteins and cholesterol on the nanoscale dynamic localization of integrins using a technique called FRET, fluorescence resonance energy transfer. FRET is used to detect the proximity of molecules at nanometer distances (1-10 nm) and can be applied in diverse ways with various microscope

configurations. FRET images obtained with such setups can be used to quantify the interactions between biomolecules within cells.

The general introduction chapter covers a broad background on topics that would place the following chapters in perspective. This chapter encompasses background topics like the composition and functions of the cell membrane, the importance of cell signaling, how some of the membrane proteins called receptors participate in cell signaling, description of a class of receptors called integrins, and clustering of integrins. The chapter also includes a literature survey of measuring protein-protein interactions using FRET. Additionally, a rigorous discussion on the theory behind FRET, the details of the instrumentation as well as various FRET equations and parameters needed when designing experiments are also included. Finally, the chapter concludes with a dissertation overview.

Cell signaling cascades recruit a many cytoplasmic proteins in the process of cellular communication. A better understanding of the interaction of these cytoplasmic proteins with integrins can provide essential cues about cell signaling. In this regard, one of the first steps would be to identify the cytoplasmic proteins that affect the integrins dynamics. The second chapter focuses on the work involved in the coupling of a biotechnology tool with FRET microscopy technique to identify key cytoplasmic proteins affecting the integrin microclustering. The chapter discusses the changes in integrins microclustering under reduced expression of several key cytoplasmic proteins. The details of the FRET technique used to measure integrin microclustering and the biotechnology technique used to reduce the expression of cytoplasmic proteins are presented in this chapter. Concomitant studies validating the reduced expression levels of cytoplasmic proteins are also included.

Cholesterol is a small lipid molecule that intercalates between the fatty acyl chains of the cell membrane lipid bilayer. It is known to maintain the membrane structure and regulate the membrane fluidity. Previous studies have shown intramembranous hydrophobic interactions between cholesterol and other membrane proteins. While chapter two identifies key cytoplasmic proteins affecting integrin microclustering, the third chapter focuses on investigating the role of cholesterol in the microclustering of integrins. Modulation of membrane cholesterol levels using cyclodextrins as well as the validation of changes in cholesterol levels using a fluorometric assay are presented in this chapter. Additionally, the measurement of subsequent changes in integrin microclustering upon cholesterol removal is discussed in this chapter. Further insights into the integrins dynamics in light of the altered membrane lipid diffusion upon alteration in the cholesterol levels is presented in this chapter. Lastly, reversibility of the process upon restoration of membrane cholesterol levels is discussed.

Chapter four provides general conclusions to the preceding chapters as well as the future prospects of the FRET based receptor microclustering measurements. Although chapter 2 and 3 are related to each other, they aim at probing the roles of two different cell components (cytoplasmic proteins and cholesterol) on the integrin microclustering. Therefore, both chapter 2 and chapter 3 have been or intended to be published separately in scientific, peer reviewed journals.

Besides the aforementioned four chapters, there are two additional projects that are not included in this dissertation. The research that goes into these two projects was performed at Iowa State University under the supervision of Prof. Marc D. Porter and Dr. Robert J. Lipert during fall-2003 to fall-2006. The first project involves the development of a

separation method, using reverse phase High Performance Liquid Chromatography (HPLC) and Size Exclusion Chromatography, to rapidly pre-screen plant extracts of *Echinacea* and *Hypericum* for drug-like compounds. The second project involved synthesizing novel Raman-active nanoconjugates made of magnetic and gold nanoparticles to improvise analysis times in immunoassays. These projects could not be included in my dissertation as per Iowa State University policies.

LITERATURE REVIEW

Cell Membrane Organization

Cell Membrane: Each one of the 100 trillion cells in our body has a 5-10 nm thick boundary enclosing and compartmentalizing both the entire cell and the organelles within them. In the absence of this frontier, human life would be impossible. In fact, defects in the boundary have been implicated in a host of diseases such as sickle cell anemia, muscular dystrophy, retinal degeneration and lysosomal storage disorder.[1-3] This frontier is a dynamic fluid-like boundary with its components continuously moving around. The basic structure of

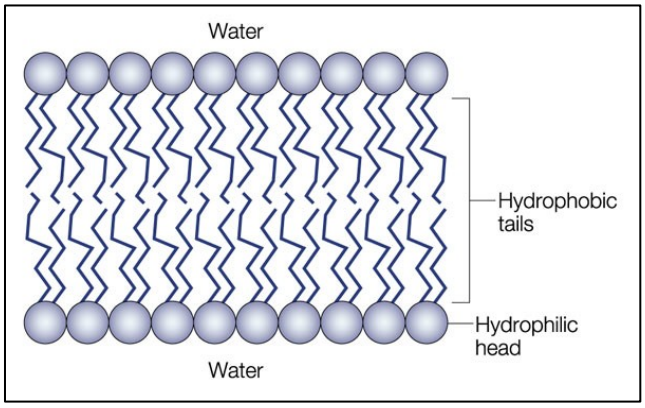

Figure 1. Structure of lipid bilayer. Blue circles represents water loving phospholipid groups and the wiggly tails represents hydrocarbon chains.

the membrane comprises the phospholipid bilayer, made up from a hydrophilic phosphate headgroups and two hydrophobic lipid tails (Figure 1).

When phospholipids are exposed to water, the hydrophobic tails from one phospholipid are pushed towards the tail from another phospholipid forming a hydrophobic inner core and a hydrophilic exterior. The membrane is further stabilized by hydrogen bonds, electrostatic attractions and van der Waals forces.

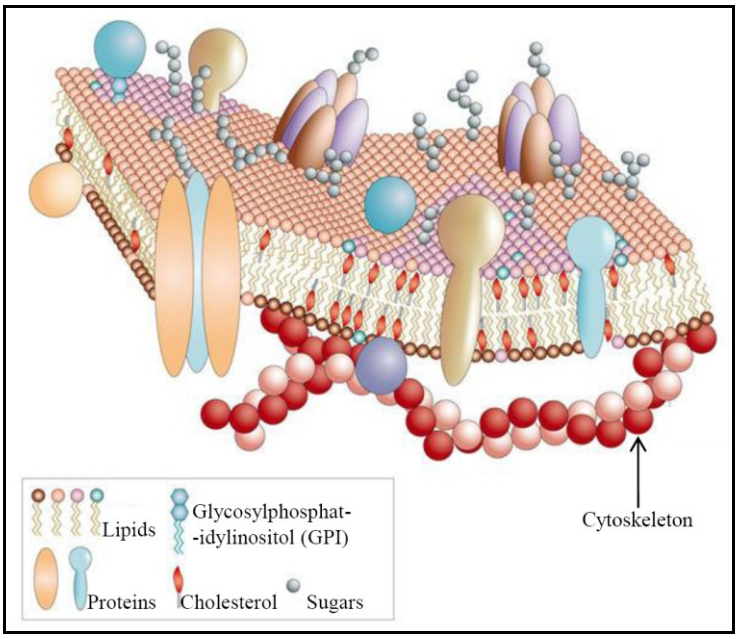

Figure 2. Diagram of the cell membrane. (adapted from Nature Publishing Group)

In addition to phospholipids, the cell membrane is composed of proteins, sterols and small molecules as depicted in Figure 2. The relative amounts of these components vary from cell to cell dictating the diverse cellular functions. The proteins in the membrane are extremely important in carrying out various functions such as glucose uptake, channeling ions, immune response, anchoring cytoskeletal filaments and cell signaling.

Cell Signaling. Signaling in cells is vital for their survival, growth, proliferation, differentiation and other basic functions.[4-6] Errors in processing the signaling events could result in various pathological conditions including cancer metastasis.[7] During signal transduction, stimuli are intercepted by cell membrane proteins called receptors that relay the information into and out of the cell by engaging a cascading complex network of signaling partners such as kinases, Ras, G proteins etc..[6, 8-10] Signal transduction is carried out by the receptors, such as integrins, through three primary mechanisms (a) binding of the extracellular ligands to the extracellular domain of the receptors causing conformational changes that is relayed into the cell interior, known as outside-in-signaling; (b) intracellular binding of proteins or other biomolecules to the cytoplasmic domain of the receptor, referred as inside-out signaling; and (c) clustering of receptors within the plasma membrane. Receptor clustering has been involved in many vital processes such as immunological synapse formation[11], actin cytoskeleton regulation[12] and leukocyte regulation[13].

Integrin Receptors. One class of receptors that are pivotal to many cell signaling events are integrins, which are heterodimeric cell membrane receptors composed of one α subunit noncovalently associated with one β subunit.[14, 15] They have been found to regulate adhesion of cells to components of the extracellular matrix and mediate signaling through both the cytoplasm and the extracellular matrix.[4] Among other functions, integrins control aspects of cell migration, developmental events, angiogenesis and have been implicated in tumorigenesis, tumor progression, and metastasis.[16-19] Both α and β subunits comprise a large extracellular domain and a short cytoplasmic domain.[14, 15] Several forms of each subunit are known to exist, and the combination of subunits controls the receptor's binding specificity and signaling properties.[20]

While the outside-in and inside-out signaling properties of integrins have been well studied[16, 21, 22], less is known about the changes in the dynamic interactions that lead to the microscale and macroscale integrin clusters within the cell membrane during cell signaling events. Because of the size, real-time dynamics of macroscale clusters can be observed using conventional optical microscopy. However, observing microscale clustering events in live cells require an unobtrusive, non diffraction limited detection technique that minimally disturbs the system. For this, FRET, a technique based on the non radiative transfer of energy

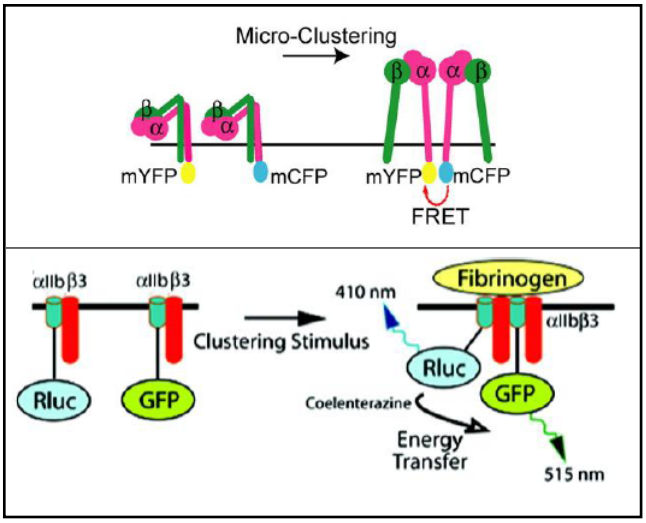

Figure 3. FRET assays to measure integrin microclustering by tagging the integrins. (adapted from references 25 & 26)

between donor and acceptor fluorophores that are in close proximity, has been used previously to measure the microscale spatial characteristics of biomolecules.[23, 24] The FRET technique is discussed in detail below. Previous experimental attempts to study microscale integrin clustering using FRET assays involved direct attachment of fluorescent probes to the integrins.[25, 26] Figure 3 (top) shows the study done by Kim M. et al where integrin subunits were cloned with either donor (mCFP) or acceptor (mYFP) fluorescent proteins. FRET was observed when the subunits were in close proximity (< 10 nm).[26]

In another study (Figure 3, bottom), the α subunit was tagged, via cloning, with either the donor (Rluc) or acceptor (GFP) proteins. The clustering of integrins was induced by external stimulus and subsequent energy transfer between the Rluc and GFP was observed when the integrins were within ~ 8 nm distance.[25]

There are two important points that must be noted when measuring FRET using the above approaches. The direct attachment of fluorescent probes to the integrins could potentially alter the properties of integrins and their interaction with other biomolecules. Secondly, if mutant integrins are to be studied, several time intensive steps of cloning the fluorescent probes to each mutant would be required.

Recently, integrin microclustering was studied using a FRET assay that precluded the need for attaching the fluorescent probes directly to the integrin and the cloning of these probes for every mutant integrin.[27] Figure 4 shows the schematic of the assay that involves

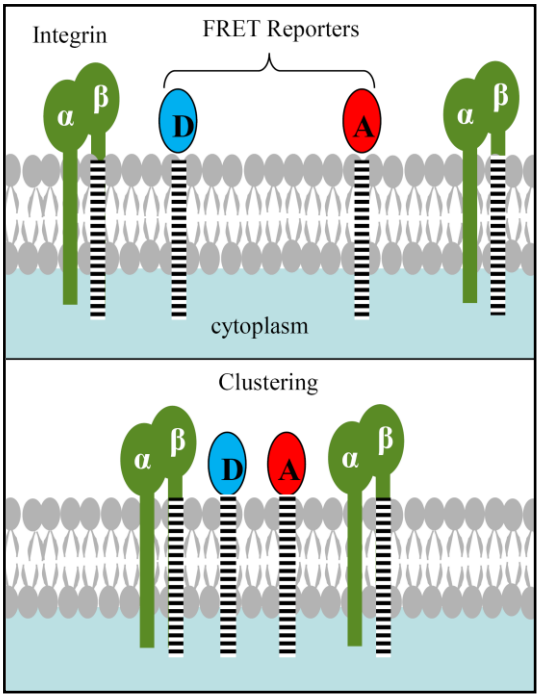

Figure 4. Schematic of the FRET assay used to measure integrin microclustering with donor and acceptor FRET reporters. (from reference 27)

FRET reporters. These reporters were constructed by cloning the extracellular donor and acceptor fluorescent proteins to the native cytoplasmic transmembrane domain of the β subunit of integrins. These reporters were co-expressed along with the integrins in the cells and found to cluster when integrins cluster. The experiments showed that utilization of FRET reporters did not alter the ligand binding affinity of integrins and the measured FRET values were independent of the reporter's expression levels. No FRET was observed in the absence of integrins. Both ligand binding affinities and FRET values increased when integrins contained mutations.

Fluorescence Resonance Energy Transfer (FRET)

Fluorescence Background. Fluorescence spectroscopy is routinely used in many applications and caters to industries such as pharmaceuticals, biotechnology, agriculture, food and beverage and environmental testing. When light is absorbed by the fluorophore, the molecule transitions from the ground electronic state to one of the higher energy state called excited electronic state (Figure 5, step 1).

There are multiple vibrational energy levels within an excited electronic state that a

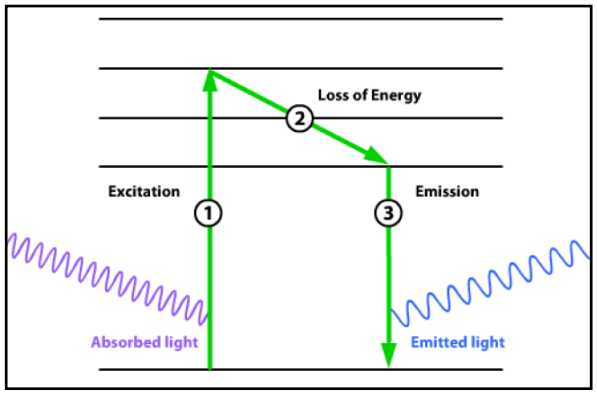

Figure 5. Energy level diagram showing the process of fluorescence spectroscopy (adapted from Invitrogen Inc.)

fluorophore can attain depending upon the excitation energy (wavelength) of the external light source. Since the fluorophore is unstable at a higher excited electronic state, it eventually adopts the lowest excited electronic state which is semi-stable (Figure 5, step 2). Next, the fluorophore returns to the ground state by emitting excess energy in the form of light (figure 5, Step 3). The emitted light is of lower energy and thus longer wavelength than the absorbed light due to the loss of energy in the transient state as shown in Figure 5, step 2. Because the excitation and emission wavelength are different, the absorbed and emitted light are detected as different colors on the visible spectrum. The fluorophore on reaching the ground state can undergo this process of absorbing and emitting light repeatedly implying that one fluorophore can generate signal multiple times thereby making fluorescence a very sensitive technique. In theory this cycle can continue indefinitely. However, in practice photobleaching often occurs because the fluorophore structure changes such that it no longer fluoresces under prolonged illumination of the sample.

Measuring Nanoscale Dynamics. In order to examine the molecular level interactions between biological entities, essential in carrying out diverse cellular functions, one of the first steps is to determine the proximity and orientation between these entities. Often the distances over which interactions between biomolecules take place are on the order of several nanometers. Although conventional wide field microscopy permits the monitoring of biochemical processes, it cannot reveal information on the order of several nanometer lengthscale due to the optical spatial resolution limits defined by the Rayleigh criterion, approximately 200 nanometers. Electron microscopy offers ample spatial resolution to address the nanoscale regime requirements. But the technique is limited in its efficacy due to the lack of precise labeling methodology. Additionally, the technique is not amenable to

imaging live cells, which provides the most information about these biochemical interactions. FRET is a technique that can solve these problems on the scale of molecular distances.

FRET Theory. FRET is used in microscopy to measure the proximity of fluorophores. It is a process by which energy is transferred from an excited donor fluorophore to a ground state acceptor fluorophore by means of long-range dipole-dipole resonance interaction. Figure 6 is the energy level diagram showing the coupled excited state

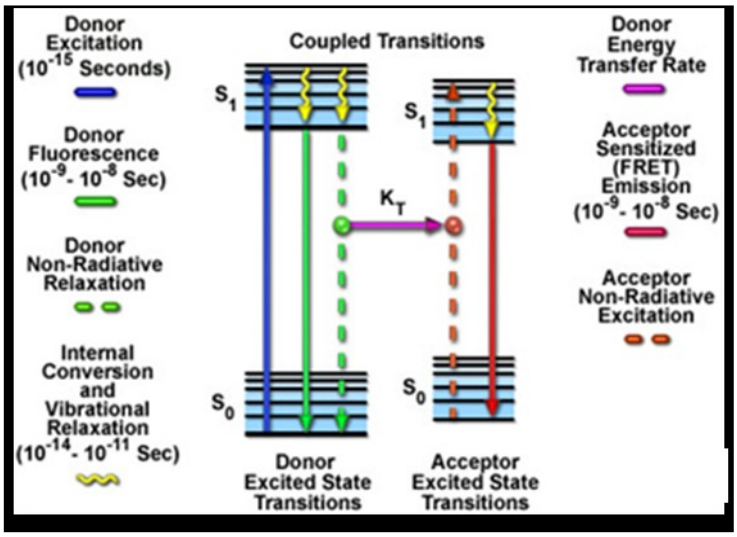

Figure 6. Energy level diagram for the FRET phenomenon (adapted from Nikon Inc.)

transitions involved between the donor emission and acceptor excitation involved in the FRET process. Vertical arrows (blue, green and red), denote excitation and emission transitions and wavy yellow arrows are the vibrational relaxation. The vertical dashed lines represent the coupled transitions as if they arise from photon-mediated electronic transitions. Energy is not transferred as a photon, rather as a coulombic charge-charge interaction between donor and acceptor molecules. The excited donor fluorophore transfers excited state energy directly to the acceptor without emitting a photon as shown by a violet arrow in

Figure 6. This results in a sensitized fluorescence that has characteristics similar to the fluorescence of the acceptor.

FRET Measurements. The efficiency of this FRET process is given by E (Equation 1), which shows the dependence of efficiency on the distance between the donor and acceptor fluorophore.[28] The efficiency varies as the inverse sixth power of the distance between the donor and acceptor.

$$E = \frac{\#\text{of quanta transferred from donor to acceptor}}{\#\text{ of quanta absorbed by donor}} = \frac{1}{1+(r/\mathrm{R_o})^6} \qquad (1)$$

Figure 7 shows the changes in FRET efficiency over the distances between a given FRET pair. Since efficiency is proportional to the distance as the inverse of sixth power, a sharp decrease in the curve over small distance is observed. $R_{o,}$ referred to as Forster radius, named after the scientist who first proposed the theory of FRET, is defined as the distance at which FRET efficiency is 50% and is the characteristic for a fluorescent donor-acceptor pair.

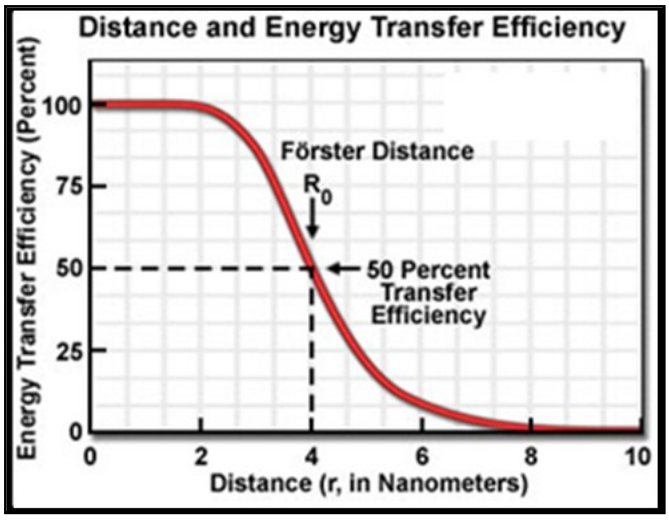

Figure 7. Shows the changes in FRET efficiency as the separation distance between a given FRET pair is changed. (adapted from Olympus America Inc.)

The efficiency is close to maxima for distances less than R_o and declines sharply for distances greater than R_o.

The FRET efficiency depends upon R_o which in turn is proportional to many parameters. Equation 3 is a mathematical relationship of R_o for an aqueous system, where K denotes the dipole orientation factor between the donor-acceptor pair, Q_d is the quantum yield of the donor, E_A is the molar absorption coefficient of the acceptor and J (λ) represents spectral overlap between the donor fluorescence and acceptor absorption.

$$R_o = \left[2.8 \times 10^{17} \times K^2 \times Q_D \times E_A \times J(\lambda) \right]^{1/6} \quad (2)$$

In order to maximize the FRET, donor and acceptor must be selected keeping these equations in mind. Thus for a higher FRET there should be a higher overlap between the donor emission spectra and acceptor excitation spectra (Figure 8), the quantum yield of donor should be high, the acceptor should have a high absorption coefficient. In addition, the transition dipoles of donor or acceptor must be oriented favorably with respect to each other. K defines the degree of orientation and can vary between 0 and 4. For most of the practical applications, K is assumed to be 2/3. [29] It is important to note that the variables given in Equation 2 govern the FRET efficiency only by the sixth power. For example, if a variable is increased by 100%, the effective change in FRET would be less than 20%.

Knowing that FRET occurs over 1-10 nm distances and is sensitive to the relative orientation of the fluorophores, FRET-based analysis is well-suited to probe the protein-protein interactions that occur between two molecules positioned within several nanometers of each other.

Measuring protein-protein interactions using FRET

Recent years has seen enormous growth in the application of FRET that includes studying the spatial distribution and assembly of protein complexes, the structure and conformations of proteins and nucleic acids, receptor ligand interaction, formation of receptor dimers, nucleic acid hybridization and many more.

G-protein coupled receptor (GPCR) is a well known protein involved in variety of cellular processes and undergoes changes, such as dimerization and oligomerization, to perform various cellular functions. FRET has been used to demonstrate the existence of GPCRs as either homo- or hetero- oligomeric complexes.[30, 31] Epidermal growth factor receptor (EGFR) is a cell surface receptor and participates in various cellular processes, for example, mediating immune response in human skin.[32] Misregulation and mutations in EGFR has been known to play a significant role in many pathological conditions including cancers.[33-35] FRET has been utilized in studying the agonist-induced dimerization of the epidermal growth factor receptor.[36-39] FRET has also been used to study the protein-induced DNA bending by measuring the changes in the energy transfer between fluorophores localized at the ends of the target DNA duplex.[40] The FRET technique has been used to study the binding of monovalent haptens to cell-bound immunoglobulinE and the dihydropyridine binding to L-type Ca^{+2}-channels.[41, 42] Hybrid formation and dissociation of oligonucleotides in living cells has been studied with the use of FRET.[43] The technique has been used to study protein-protein interactions in plant systems as well.[44]

FRET instrumentation

A standard fluorescence microscope can be used to measure FRET in a simple, fast and non-destructive way. [45-48] FRET can be easily calculated using Equation 3, where I_{DA} represents intensity when donor is excited and emission of acceptor is measured and I_{DD} represents intensity when donor is excited and emission of donor is measured.

$$FRET = \frac{I_{DA}}{I_{DD}} \tag{3}$$

However, there are two important factors that should be accounted for before reasonable FRET can be measured. Equation 2 shows the strong dependence of FRET on the overlap between the emission of donor and the excitation of acceptor. When ensuring a substantial overlap between donor fluorescence and acceptor excitation, in all the practical applications there is invariably some contamination of the I_{DA} intensity that can occur (Figure 8).

This happens due to the direct excitation of the acceptor along with the donor (overlap of A_{abs} and D_{abs} curves) and a fraction of donor fluorescence leaking into detection

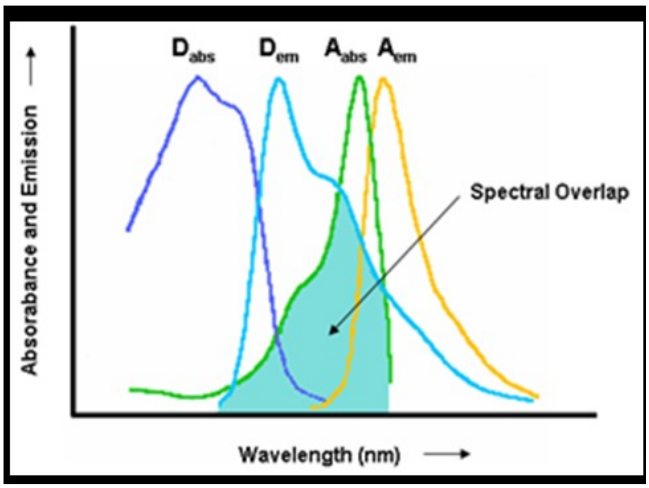

Figure 8. Excitation and emission spectra of a typical donor-acceptor pair used in FRET measurements. (adapted from reference 44)

channel for the acceptor fluorescence (overlap of D_{em} and A_{em} curves)**.** In addition, there are undesired spectral overlap of acceptor fluorescence with the acceptor excitation (overlap of A_{em} and A_{abs} curves) and the donor excitation (overlap of A_{em} and D_{abs} curves).

Bleedthrough Factors. The FRET measurements need to account for these contaminations referred to as bleedthrough or crosstalk. In that regard combination of optical filters and samples (acceptor only, donor only) are used to obtain images and the bleedthrough factors can be determined using the following equations.

$$a = \frac{I_{DA(A)}}{I_{AA(A)}} \tag{4}$$

$$b = \frac{I_{DD(A)}}{I_{AA(A)}} \tag{5}$$

$$c = \frac{I_{AA(D)}}{I_{DD(D)}} \tag{6}$$

$$d = \frac{I_{DA(D)}}{I_{DD(D)}} \tag{7}$$

The term in parentheses represents what sample is present, whether the sample contains only donor (D) or only acceptor (A). The factor 'a' represents the acceptor bleedthrough in FRET filter channel; the factor 'b' represents the acceptor bleedthrough in Donor filter channel; the factor 'c' represents the donor bleedthrough in Acceptor filter channel. The factor 'd' represents donor bleedthrough in FRET filter channel. The experimental setup should be such that these factors are as small as possible minimizing the bleedthrough. These bleedthrough factors can be used to correct the FRET equation, which will be discussed in detail later.

FRET Indices. Besides bleedthrough factors, donor-to-acceptor stoichiometry in the sample needs to be considered when measuring FRET. Typically tens to hundreds of samples (e.g. cells) are analyzed to get a statistically significant FRET. Not all the cells maintain the same ratio of donor-acceptor stoichiometry. In order to account for this variation in the concentration of fluorophore as well as the bleedthrough factors, several user-defined FRET indices have been developed.[46, 49-53] The numerator of these FRET indices contains correction term for bleedthrough the denominator renders the whole index independent of the fluorophore concentration. Some of the commonly user-defined FRET indices developed by different researchers as per their experimental conditions are given below.

$$F_c/D = \frac{I_{DA} - aI_{AA} - dI_{DD}}{I_{DD}} \tag{8}$$

$$F_a/D = \frac{I_{DA} - aI_{AA}}{I_{DD}} \tag{9}$$

$$F_c/A = \frac{I_{DA} - aI_{AA} - dI_{DD}}{I_{AA}} \tag{10}$$

$$F_d/A = FR \times a = \frac{I_{DA} - dI_{DD}}{I_{AA}} \tag{11}$$

$$FRETN = \frac{I_{DA} - aI_{AA} - dI_{DD}}{G \times I_{DD} \times I_{AA}} \tag{12}$$

$$FRET = \frac{I_{DA} - aI_{AA} - dI_{DD}}{\sqrt{I_{DD} \times I_{AA}}} \tag{13}$$

Equations 8-9 represent the indices where donors denominate the indices[51-53]. Equations 10-11 represent group of indices[49, 50] where acceptor concentration denominates

the index and Equations 12-13 represent the indices[45, 46] where both the donor and acceptor concentration denominates the index.

***Fluorescence Microscope Set-up*:** A schematic of the fluorescence microscope in our laboratory is shown in Figure 9. The set up consists of an inverted standard Nikon TE2000 microscope that can be easily configured to measure FRET. The light source is a mercury lamp and the filters correspond to the fluorescent molecules used in the study. The light enters into the microscope and after travelling through the excitation filter, a select wavelength band is reflected by the dichroic and impinges upon the sample through the objective.

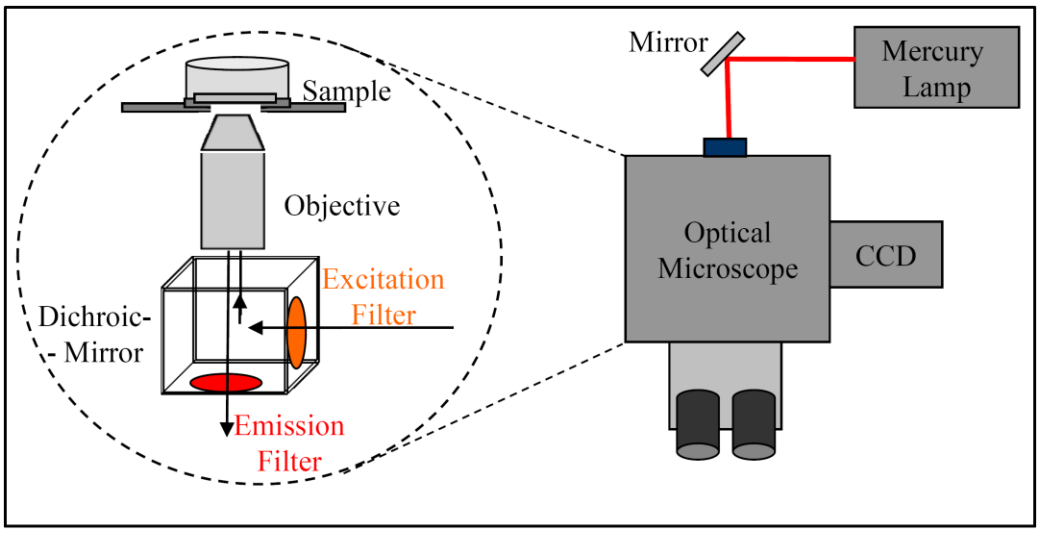

Figure 9. Diagram of the fluorescence microscope used to collect the FRET data. The sample illumination and collection optics is shown in the dashed circle.

The same objective is used to collect the fluorescence signal from the sample as well. The dichroic mirror reflects the excitation wavelengths when light is going towards the sample and transmit the emission wavelengths when light is coming from the sample. The emitted signal transmitting through the dichroic passes through the emission filter and

reaches the detector. A charged coupled device (CCD) is used as a detector to capture the light coming out of the emission filter. The software ImageJ is used for collecting and later analyzing the data to get a FRET value. The bleedthrough factors are calculated before any FRET data can be computed. Cells expressing only donor and only acceptor were used to collect the data. The values of bleedthrough factors have been discussed in detail in the chapter 2.

DISSERTATION ORGANIZATION

This dissertation is primarily focused on developing methods to measure integrin microclustering. Traditionally, integrin microclustering has been measured using FRET, by attaching fluorescent tags directly to the integrins.[25, 26] This approach could potentially affect integrins' properties such as its diffusion and its clustering within the plasma membrane. Moreover, the above methodology would require time intensive cloning steps to separately tag each integrin mutants. A recent approach overcame the above mentioned problems and demonstrated the utility of a novel FRET assay format in measuring the integrin microclustering.[27]

The aforementioned FRET assay format can be further developed to relate the integrin microclustering with the signaling events that involve intracellular proteins and plasma membrane cholesterol. The following two research chapters, presented as separate manuscripts, describe the FRET assay development to decipher the relationship of integrin microclustering with intracellular proteins and cholesterol.

Chapter 2 presents the coupling the FRET based imaging with the RNAi technique to identify key cytoplasmic proteins that affect the integrin microclustering. Chapter 3 discusses the measurement of integrin microclustering and lipid diffusion under altered plasma membrane cholesterol levels. In chapter 4, the dissertation concludes with a summation of the current work and a look at the future directions.

REFERENCES:

(1) Covas, D. T.; de Lucena Angulo, I.; Vianna Bonini Palma, P.; Zago, M. A. (2004) Effects of hydroxyurea on the membrane of erythrocytes and platelets in sickle cell anemia, *Haematologica*, 89, 273-280.

(2) McNeil, P. L.; Steinhardt, R. A. (2003) Plasma membrane disruption: repair, prevention, adaptation, *Annu Rev Cell Dev Biol*, 19, 697-731.

(3) Seabra, M. C.; Brown, M. S.; Goldstein, J. L. (1993) Retinal degeneration in choroideremia: deficiency of rab geranylgeranyl transferase, *Science*, 259, 377-381.

(4) Giancotti, F. G.; Ruoslahti, E. (1999) Integrin signaling, *Science*, 285, 1028-1032.

(5) McCoy, M. K.; Tansey, M. G. (2008) TNF signaling inhibition in the CNS: implications for normal brain function and neurodegenerative disease, *J Neuroinflammation*, 5, 45.

(6) Subauste, M. C.; Pertz, O.; Adamson, E. D.; Turner, C. E.; Junger, S.; Hahn, K. M. (2004) Vinculin modulation of paxillin-FAK interactions regulates ERK to control survival and motility, *J Cell Biol*, 165, 371-381.

(7) Sirvent, A.; Benistant, C.; Roche, S. (2008) Cytoplasmic signalling by the c-Abl tyrosine kinase in normal and cancer cells, *Biol Cell*, 100, 617-631.

(8) Fehrenbacher, N.; Bar-Sagi, D.; Philips, M. (2009) Ras/MAPK signaling from endomembranes, *Mol Oncol*, 3, 297-307.

(9) Young, A.; Lyons, J.; Miller, A. L.; Phan, V. T.; Alarcon, I. R.; McCormick, F. (2009) Ras signaling and therapies, *Adv Cancer Res*, 102, 1-17.

(10) Stryer, L.; Bourne, H. R. (1986) G proteins: a family of signal transducers, *Annu Rev Cell Biol*, 2, 391-419.

(11) Saito, T.; Yokosuka, T. (2006) Immunological synapse and microclusters: the site for recognition and activation of T cells, *Curr Opin Immunol*, 18, 305-313.

(12) Vicente-Manzanares, M.; Sanchez-Madrid, F. (2004) Role of the cytoskeleton during leukocyte responses, *Nat Rev Immunol*, 4, 110-122.

(13) Van Kooyk, Y.; Figdor, C. G. (2000) Avidity regulation of integrins: the driving force in leukocyte adhesion, *Curr Opin Cell Biol*, 12, 542-547.

(14) Adair, B. D.; Yeager, M. (2007) Electron microscopy of integrins, *Methods Enzymol*, 426, 337-373.

(15) Xiong, J. P.; Goodman, S. L.; Arnaout, M. A. (2007) Purification, analysis, and crystal structure of integrins, *Methods Enzymol*, 426, 307-336.

(16) Sastry, S. K.; Horwitz, A. F. (1993) Integrin cytoplasmic domains: mediators of cytoskeletal linkages and extra- and intracellular initiated transmembrane signaling, *Current Opinion in Cell Biology*, 5, 819-831.

(17) Shimaoka, M.; Takagi, J.; Springer, T. A. (2002) Conformational regulation of integrin structure and function, *Annu Rev Biophys Biomol Struct*, 31, 485-516.

(18) Mizejewski, G. J. (1999) Role of integrins in cancer: survey of expression patterns, *Proc Soc Exp Biol Med*, 222, 124-138.

(19) Moschos, S. J.; Drogowski, L. M.; Reppert, S. L.; Kirkwood, J. M. (2007) Integrins and cancer, *Oncology (Williston Park)*, 21, 13-20.

(20) Gotwals, P. J.; Paine-Saunders, S. E.; Stark, K. A.; Hynes, R. O. (1994) Drosophila integrins and their ligands, *Curr Opin Cell Biol*, 6, 734-739.

(21) Ginsberg, M. H.; Du, X.; Plow, E. F. (1992) Inside-out integrin signalling, *Curr Opin Cell Biol*, 4, 766-771.

(22) Martin-Bermudo, M. D.; Brown, N. H. (1996) Intracellular signals direct integrin localization to sites of function in embryonic muscles, *J Cell Biol*, 134, 217-226.

(23) Selvin, P. R. (2000) The renaissance of fluorescence resonance energy transfer, *Nat Struct Biol*, 7, 730-734.

(24) Eidne, K. A.; Kroeger, K. M.; Hanyaloglu, A. C. (2002) Applications of novel resonance energy transfer techniques to study dynamic hormone receptor interactions in living cells, *Trends Endocrinol Metab*, 13, 415-421.

(25) Buensuceso, C.; de Virgilio, M.; Shattil, S. J. (2003) Detection of integrin alpha IIbbeta 3 clustering in living cells, *J Biol Chem*, 278, 15217-15224.

(26) Kim, M.; Carman, C. V.; Yang, W.; Salas, A.; Springer, T. A. (2004) The primacy of affinity over clustering in regulation of adhesiveness of the integrin {alpha}L{beta}2, *J Cell Biol*, 167, 1241-1253.

(27) Smith, E. A.; Bunch, T. A.; Brower, D. L. (2007) General in vivo assay for the study of integrin cell membrane receptor microclustering, *Anal Chem*, 79, 3142-3147.

(28) Clegg, R. M. (1995) Fluorescence resonance energy transfer, *Curr Opin Biotechnol*, 6, 103-110.

(29) Stryer, L.; Haugland, R. P. (1967) Energy transfer: a spectroscopic ruler, *Proc Natl Acad Sci U S A*, 58, 719-726.

(30) Angers, S.; Salahpour, A.; Bouvier, M. (2002) Dimerization: an emerging concept for G protein-coupled receptor ontogeny and function, *Annu Rev Pharmacol Toxicol*, 42, 409-435.

(31) Gomes, I.; Jordan, B. A.; Gupta, A.; Rios, C.; Trapaidze, N.; Devi, L. A. (2001) G protein coupled receptor dimerization: implications in modulating receptor function, *J Mol Med*, 79, 226-242.

(32) Sorensen, O. E.; Thapa, D. R.; Roupe, K. M.; Valore, E. V.; Sjobring, U.; Roberts, A. A.; Schmidtchen, A.; Ganz, T. (2006) Injury-induced innate immune response in human skin mediated by transactivation of the epidermal growth factor receptor, *J Clin Invest*, 116, 1878-1885.

(33) Kuan, C. T.; Wikstrand, C. J.; Bigner, D. D. (2001) EGF mutant receptor vIII as a molecular target in cancer therapy, *Endocr Relat Cancer*, 8, 83-96.

(34) Paez, J. G.; Janne, P. A.; Lee, J. C.; Tracy, S.; Greulich, H.; Gabriel, S.; Herman, P.; Kaye, F. J.; Lindeman, N.; Boggon, T. J.; Naoki, K.; Sasaki, H.; Fujii, Y.; Eck, M. J.;

Sellers, W. R.; Johnson, B. E.; Meyerson, M. (2004) EGFR mutations in lung cancer: correlation with clinical response to gefitinib therapy, *Science*, 304, 1497-1500.

(35) Walker, F.; Abramowitz, L.; Benabderrahmane, D.; Duval, X.; Descatoire, V.; Henin, D.; Lehy, T.; Aparicio, T. (2009) Growth factor receptor expression in anal squamous lesions: modifications associated with oncogenic human papillomavirus and human immunodeficiency virus, *Hum Pathol*, 40, 1517-1527.

(36) Brockhoff, G.; Heiss, P.; Schlegel, J.; Hofstaedter, F.; Knuechel, R. (2001) Epidermal growth factor receptor, c-erbB2 and c-erbB3 receptor interaction, and related cell cycle kinetics of SK-BR-3 and BT474 breast carcinoma cells, *Cytometry*, 44, 338-348.

(37) Gadella, T. W., Jr.; Jovin, T. M. (1995) Oligomerization of epidermal growth factor receptors on A431 cells studied by time-resolved fluorescence imaging microscopy. A stereochemical model for tyrosine kinase receptor activation, *J Cell Biol*, 129, 1543-1558.

(38) Nagy, P.; Bene, L.; Balazs, M.; Hyun, W. C.; Lockett, S. J.; Chiang, N. Y.; Waldman, F.; Feuerstein, B. G.; Damjanovich, S.; Szollosi, J. (1998) EGF-induced redistribution of erbB2 on breast tumor cells: flow and image cytometric energy transfer measurements, *Cytometry*, 32, 120-131.

(39) Verveer, P. J.; Wouters, F. S.; Reynolds, A. R.; Bastiaens, P. I. (2000) Quantitative imaging of lateral ErbB1 receptor signal propagation in the plasma membrane, *Science*, 290, 1567-1570.

(40) Dragan, A. I.; Privalov, P. L. (2008) Use of fluorescence resonance energy transfer (FRET) in studying protein-induced DNA bending, *Methods Enzymol*, 450, 185-199.

(41) Berger, W.; Prinz, H.; Striessnig, J.; Kang, H. C.; Haugland, R.; Glossmann, H. (1994) Complex molecular mechanism for dihydropyridine binding to L-type Ca(2+)-channels as revealed by fluorescence resonance energy transfer, *Biochemistry*, 33, 11875-11883.

(42) Kubitscheck, U.; Kircheis, M.; Schweitzer-Stenner, R.; Dreybrodt, W.; Jovin, T. M.; Pecht, I. (1991) Fluorescence resonance energy transfer on single living cells. Application to binding of monovalent haptens to cell-bound immunoglobulin E, *Biophys J*, 60, 307-318.

(43) Sixou, S.; Szoka, F. C., Jr.; Green, G. A.; Giusti, B.; Zon, G.; Chin, D. J. (1994) Intracellular oligonucleotide hybridization detected by fluorescence resonance energy transfer (FRET), *Nucleic Acids Res*, 22, 662-668.

(44) Bhat, R. A.; Lahaye, T.; Panstruga, R. (2006) The visible touch: in planta visualization of protein-protein interactions by fluorophore-based methods, *Plant Methods*, 2, 12.

(45) Gordon, G. W.; Berry, G.; Liang, X. H.; Levine, B.; Herman, B. (1998) Quantitative fluorescence resonance energy transfer measurements using fluorescence microscopy, *Biophys J*, 74, 2702-2713.

(46) Xia, Z.; Liu, Y. (2001) Reliable and global measurement of fluorescence resonance energy transfer using fluorescence microscopes, *Biophys J*, 81, 2395-2402.

(47) Chen, H.; Puhl, H. L., 3rd; Koushik, S. V.; Vogel, S. S.; Ikeda, S. R. (2006) Measurement of FRET efficiency and ratio of donor to acceptor concentration in living cells, *Biophys J*, 91, L39-41.

(48) Zal, T.; Gascoigne, N. R. (2004) Photobleaching-corrected FRET efficiency imaging of live cells, *Biophys J*, 86, 3923-3939.

(49) Erickson, M. G.; Alseikhan, B. A.; Peterson, B. Z.; Yue, D. T. (2001) Preassociation of calmodulin with voltage-gated Ca(2+) channels revealed by FRET in single living cells, *Neuron*, 31, 973-985.

(50) Jiang, X.; Sorkin, A. (2002) Coordinated traffic of Grb2 and Ras during epidermal growth factor receptor endocytosis visualized in living cells, *Mol Biol Cell*, 13, 1522-1535.

(51) Miyawaki, A.; Griesbeck, O.; Heim, R.; Tsien, R. Y. (1999) Dynamic and quantitative Ca2+ measurements using improved cameleons, *Proc Natl Acad Sci U S A*, 96, 2135-2140.

(52) Vanderklish, P. W.; Krushel, L. A.; Holst, B. H.; Gally, J. A.; Crossin, K. L.; Edelman, G. M. (2000) Marking synaptic activity in dendritic spines with a calpain substrate exhibiting fluorescence resonance energy transfer, *Proc Natl Acad Sci U S A*, 97, 2253-2258.

(53) Zal, T.; Zal, M. A.; Gascoigne, N. R. (2002) Inhibition of T cell receptor-coreceptor interactions by antagonist ligands visualized by live FRET imaging of the T-hybridoma immunological synapse, *Immunity*, 16, 521-534.

CHAPTER 2: IDENTIFYING CYTOPLASMIC PROTEINS THAT AFFECT RECEPTOR CLUSTERING USING FLUORESCENCE RESONANCE ENERGY TRANSFER AND RNA INTERFERENCE

A paper published in Analytical and Bioanalytical Chemistry 2009, 395 (7), 2303-2311*

Deepak Dibya, Suzanne Sander and Emily A. Smith

ABSTRACT

Unraveling the complex, dynamic organization of the cell membrane can provide vital information about many aspects of cellular functions. Reported herein is a method for identifying cytoplasmic proteins that affect cell membrane protein organization. RNA interference (RNAi) is used to reduce the expression of select cytoplasmic proteins and a fluorescence resonance energy transfer (FRET) assay is used to measure changes in receptor microclustering. The advantage of this assay is that it does not require attaching fluorescent tags to the receptor. A change in energy transfer after reducing the expression of a cytoplasmic protein provides information about the protein's role in altering receptor organization. As a demonstration of the method, cytoplasmic

---

proteins involved in integrin microclustering have been identified. The cytoplasmic proteins targeted in this study include: dreadlock, integrin-linked kinase, paxillin, steamer duck, vinculin, rhea, focal adhesion kinase, and actin 42A.Reducing the expression of vinculin, paxillin, rhea, and focal adhesion kinase increased integrin microclustering, as measured by an increase in energy transfer in cells expressing αPS2CβPS integrins. No change in integrin microclustering was measured in a control cell line. Integrin mutants exhibited different microclustering properties compared to the wild-type integrins after reducing the expression of the listed cytoplasmic proteins. The results demonstrate the utility of this assay format, and provide insight into the function of cytoplasmic proteins in integrin microclustering.

INTRODUCTION

A dynamic flow of information between the extracellular and intracellular environments of a cell is required for survival, growth, proliferation, differentiation, and other basic functions (1). The primary signal transducers are receptor cell membrane proteins. Receptors transmit information through three primary mechanisms: (a) binding extracellular ligands; (b) engaging a cascading network of intracellular signaling partners; and (c) clustering within the membrane. Several analytical techniques, such as co-immunoprecipitation, surface plasmon resonance, affinity chromatography, and two-hybrid systems, are used to measure the interactions of receptors with their intracellular and extracellular signaling partners (2).

Observing nanoscale receptor organization in live cells requires a non-invasive detection technique that is not subject to diffraction-limited spatial resolution. Fluorescence resonance energy transfer (FRET) is ideally suited for measuring nanoscale membrane organization (3). FRET studies of receptor microclustering have primarily used the direct attachment of donor and acceptor fluorescent proteins to the extracellular or intracellular domain of the membrane protein (4, 5). Direct fluorophore attachment could potentially alter the receptor's clustering properties, as well as their interaction with other biomolecules. This experimental approach also requires time-consuming protein cloning steps to attach the donor and acceptor fluorescent proteins to each protein mutant.

A recently reported FRET assay overcomes these problems (6). Shown in Fig. 1 is a schematic of this FRET assay, which is used to measure the microclustering of αPS2CβPS integrins. Integrins are heterodimeric cell membrane receptors that are pivotal to many cellular functions, and mediate signaling through both the cytoplasm and the extracellular matrix (1, 7). The integrin microclustering assay used FRET reporter peptides that were expressed in cells along with integrins. The FRET reporter peptides contain the integrins' β subunit cytoplasmic and transmembrane domain fused to donor or acceptor fluorescent proteins. A previous report showed that the β cytoplasmic and transmembrane region is sufficient for clustering with full-length integrin *in vivo* (8). The donors and acceptors were a monomeric yellow fluorescent protein variant mVenus and a monomeric dsRED variant mCherry, respectively. Hereafter, the term FRET reporters refers to a population of donor transmembrane peptides and a separate population of acceptor transmembrane peptides.

The fusion of fluorescent proteins to the β subunit transmembrane and cytoplasmic domain to generate FRET reporters allows the donor and acceptor fluorophores to take part in integrin clustering. When integrins cluster, so do the FRET reporters. This results in a reduced average donor–acceptor separation distance and an increase in observed FRET. The use of FRET reporters eliminates the need to attach the donor and acceptor directly to the integrin, and does not require numerous steps to clone donor and acceptor fluorescent groups to each integrin mutant. The integrin diffusion and clustering properties are not altered in this assay format since the fluorescent proteins are not directly attached to the integrins. The reporters: (a) do not contain ligand-binding domains so there is no competition between the integrin and FRET reporters for ligand; (b) do not alter the integrins' ligand binding affinity; and (c) do not produce energy transfer in the absence of integrins (6). A set of FRET control peptides contained the same fluorescent proteins cloned to the transmembrane and cytoplasmic domains of a protein (mouse CD2) with no sequence homology in S2 cells. The assay has been used to measure receptor clustering, but it has not been demonstrated that it can be used to relate intracellular binding events with receptor clustering. This would enable a more detailed molecular understanding of cell membrane organization.

Reported herein is a systematic approach for identifying cytoplasmic proteins that affect receptor microclustering. The method uses the FRET assay described above along with RNA interference (RNAi) to reduce the expression of select proteins. Changes in energy transfer are measured to identify proteins that affect integrin microclustering. The cytoplasmic proteins that have been studied include: rhea (9), vinculin (10), paxillin (10),

focal adhesion kinase (10), steamer duck (11), dreadlock (11), integrin-linked kinase (11)and actin42A (12).

EXPERIMENTAL

S2 cell culture

Transformed *Drosophila* S2 cells were cultured in Shields and Sang M3 insect media (M3, Sigma) supplemented with 10% fetal bovine serum (Irvine Scientific), 12.5 mM streptomycin, 36.5 mM penicillin, and 0.2 μM methotrexate (Fisher Scientific) in a 22°C incubator. Cells were co-transfected to express integrin subunits and FRET reporters or FRET controls. Complete protein sequences for the FRET controls, FRET reporters containing mVenus or mCherry fluorescent proteins (6), wild-type and mutant integrin subunits (6, 13-15)have been published elsewhere. All endogenous proteins contain the heat shock promoter.

dsRNA synthesis

Double-stranded RNA (dsRNA) was generated using published protocols with minor modifications, as noted below (16). Polymerase chain reactions were used to amplify 200 to 700-bp DNA sequences from S2 genomic DNA. The primer sequences can be identified from the information listed in Table 1. Both forward and reverse primers contained the T7 RNA polymerase promoter binding site (TAATACGACTCACTATAGGG). The polymerase

chain reaction products were analyzed using 1% agarose gel electrophoresis and were subsequently used as templates for RNA synthesis with the MEGASCRIPT T7 Transcription Kit (Ambion, Austin, TX) to produce single stranded RNA. The single-stranded RNA products were ethanol-precipitated and re-suspended in water. dsRNAs was generated by incubating the solution at 65°C for 30 min followed by slow cooling to room temperature, and analyzed by 1% agarose gel electrophoresis to ensure that only the desired product was obtained. The concentration was measured using the solution absorbance at 280 nm and the solutions were diluted to 1 μg/μL. The dsRNA solution was stored at −20°C until subsequent use.

RNAi treatment

Detailed protocols have been previously published, and were followed with changes noted below (16, 17). Approximately 6×10^5 cells were plated per well in a 12-well cell culture dish. Cells were rinsed with 600 μL of serum-free M3 medium, and 300 μL of serum-free media was added to each well. Ten micrograms of dsRNA was added directly to each well, and the cells were incubated for 60 min in a 22°C incubator followed by addition of 300 μL M3 media containing 20 % fetal bovine serum. The cells were incubated at 22°C for an additional 4 days. Reduced expression of the target protein has been reported up to 5 days after RNAi treatment.

FRET assay

After RNAi treatment and 4 days of incubation, cells were transferred from the cell culture dish to a polypropylene tube and heat-shocked for 30 min at 36°C to induce the expression of integrins and FRET reporters or controls. Cells were then placed in a 22°C incubator for 3 h to achieve maximum protein expression. The cells were centrifuged at approximately 600×g, the pellet was resuspended in serum-free medium and the concentration was adjusted to 3×10^5 cells/mL. The cells were placed on a RBB-tiggrin coated substrate and allowed to spread for 1 h in the serum-free medium. Details about the RBB-tiggrin substrate are provided in the supplemental information. The medium was replaced with 20 mM BES Tyrodes buffer prior to analysis. The analysis was completed within 1.25 h of replacing the medium with BES buffer to ensure cell viability. At least three RNAi treatments were performed for every targeted protein and every cell line. The cells were analyzed using a ×60 magnification, numerical aperture 0.95 objective and a Eclipse TE2000U microscope (Nikon) with low-intensity mercury lamp illumination. The images were captured with a Coolsnap CCD camera (Roper Scientific Photometrics, Pleasanton, CA) using the program Micromanager, which operates within the ImageJ 1.37v software. The camera was set to bin 8×8 pixels. Images were captured utilizing three different filter sets for each cell analyzed: (a) donor filter set (excitation 500/20 nm, emission 535/30 nm), (b) acceptor filter set (excitation 545/30 nm, emission 620/60 nm), and (c) donor excitation filter with acceptor emission filter (FRET filters). The exposure time for the FRET, acceptor and donor images were 12, 6, and 6 s, respectively. The Drosophila S2 cells did not move in the time it took to capture the three images.

Data and statistical analysis

Data was analyzed using the program ImageJ, and a plugin that was developed with the Java platform. The plug-in calculates a FRET value for each pixel in the image. After the appropriate background value is subtracted from each pixel, a FRET value is calculated using the equation:

$$FRET = \frac{I_{DA} - a(I_{AA} - cI_{DD}) - d(I_{DD} - bI_{AA})}{\sqrt{I_{DD}I_{AA}}} \quad (1)$$

where I_{DA}, I_{AA}, and I_{DD} are intensities obtained from the images with the FRET, acceptor, and donor filters, respectively. The factors a, b, c, and d account for bleedthrough of: acceptor into the FRET filters, acceptor into the donor filters, donor into the acceptor filters, and donor into the FRET filters, respectively. All four bleedthrough factors were non-zero on the microscope system used in these studies. Further discussion of the bleedthrough factors can be found in the supplemental information. There are numerous alternative FRET equations that can be used in conjunction with this methodology (18-20). Equation 1 is suitable for measuring increases or decreases in FRET efficiency after RNAi treatment.

All statistical analyses were performed using the application JMP 7 (SAS Institute Inc, Cary, USA), with statistical consulting through the Iowa State University Department of Statistics. For every reported value, at least 100 cells from three replicate experiments were analyzed. The raw FRET data are not normally distributed, which means that statistical tests such as the t-test cannot be used on the raw data. The data were transformed to a normal

distribution by taking the natural log of the raw data, and the means were calculated from the transformed data. The Welch test was used to compare the means of the log-transformed data since the data sets were determined to have unequal variances by Levene's test. Results of the Welch Test are reported as p values, which are a measure of the significance of the statistical tests. A p value lower than 0.05 provides evidence that the energy transfer measured for the RNAi treatment data set is altered compared to the no RNAi treatment data set. A p value greater than 0.05 does not provide the statistical evidence to say there is a difference between the data sets. In order to report the mean value in the original data scale, the antilog of the mean of the log-transformed data was taken. Further information on these methods can be found in statistics textbooks (21).

RESULTS AND DISCUSSION

FRET assay

Figure 1 shows a schematic of the FRET assay used to study the effect of cytoplasmic proteins on integrin microclustering in live cells. A set of three images is captured for each cell: donor, acceptor, and FRET. Figure 2 shows a series of images used to calculate energy transfer in cells expressing wild-type integrins and FRET reporters. Using a home-built plug-in for the program ImageJ, an energy transfer value is calculated for each pixel in the image using Eq. 1. A region of interest (ROI) is generated for each cell. Specifically, background regions and regions corresponding to the nuclear and perinuclear regions are excluded from the analysis. Intense fluorescence is observed in these regions, corresponding to FRET

reporters inside the cell. The signal from the nuclear and perinuclear regions interferes with the measurement of integrin clustering in the cell membrane. An example ROI is shown in Fig. 2. An average value is calculated from all the pixels in a ROI to generate a single FRET value for each cell. The distribution of FRET values for all pixels in the example ROI is provided in the supplemental information (Supplemental Figure S1).In order to ensure that a suitable ROI can be defined, only spread cells with diameters greater than 20 μm are analyzed. The average diameter of the spread cells analyzed by FRET did not statistically differ for any of the cell lines or RNAi treatments (data not shown).

In order to measure intracellular events that affect integrin clustering, without interference from extracellular ligand binding, minimizing extracellular signaling is desirable. To accomplish this, cells were spread on a surface with low ligand density. The extracellular ligand for the integrins used in these studies (RBB-tiggrin) is a 53 amino acid protein. Assuming RBB-tiggrin's size is 2 nm×3 nm (22), and all the RBB-tiggrin adheres to the glass slide, approximately 3% to 5% of the 30 mm^2 glass slide is covered at the ligand density used in these studies. Bovine serum albumin is used to cover the remaining glass surface to inhibit non-specific cell binding to the glass. A surface with no ligand, coated only with bovine serum albumin, would completely eliminate extracellular signaling events. However, cell attachment and cell spreading were significantly reduced when no ligand was present. The reduced cell spreading in the absence of ligand precluded FRET measurements on a large-enough number of cells to provide statistically significant results.

Energy transfer was measured in cells expressing integrins and FRET reporter peptides or FRET control peptides. The integrins were either wild-type or mutants. Two

well-characterized integrin mutants that are studied have different ligand-binding affinities compared to wild-type integrin. The mutant αanaβ integrins contain a two-point mutation in the cytoplasmic domain of the α subunit. This mutation is considered to mimic signal transduction from inside to outside the cell (23). The mutant αβV409D integrins contain a single-point mutation in the extracellular domain of the β subunit that mimics signal transduction from outside to inside the cell (24).

At 3% to 5% ligand surface densities, statistically similar energy transfer values were measured for three cell lines expressing wild-type or mutant (αanaβ, αβV409D) integrins and FRET reporters (Table 2). This indicates similar levels of FRET reporter microclustering for the three cell lines at these experimental conditions. Similar energy transfer values are also obtained for cells expressing wild type integrins and FRET reporters compared to cells expressing wild-type integrins and FRET controls (Table 2). Three factors must be considered to interpret these results: (1) the energy transfer values are above the detection limit for the microscope system; (2) the total energy transfer measured is a result of integrin-specific FRET reporter clustering and non-integrin-specific FRET reporter clustering from many sources; (3) at high ligand densities, higher energy transfer values are measured for cells expressing FRET reporters compared to cells expressing FRET controls. At 3% to 5% ligand densities, the energy transfer reported in Table 2 (αβ FRET Reporters, αanaβ FRET Reporters, αβV409D FRET Reporters) is the result of non-integrin-specific microclustering of the FRET reporters. Integrin-specific clustering would be detected as an increase in energy transfer for the cell line expressing FRET reporters relative to the cell line expressing FRET controls, which is observed at high ligand densities (6). It is not possible to say that no

integrin microclustering occurs at 3% to 5% ligand density. Integrin microclustering that causes an insignificant increase in FRET reporter microclustering relative to the non-integrin-specific microclustering of the FRET reporter may be present. The data presented in Table 2 is referred to as the no RNAi treatment data in the following discussion.

RNAi transfection

RNAi was used to reduce the expression of select cytoplasmic proteins. The proteins targeted in this work are highlighted gray in Fig. 1. These proteins are known to be involved in integrin-signaling complexes, and are expressed in S2 cells as reported in the FLIGHT mRNA microarray expression database (24) and PeptideAtlas mass spectrometry proteomics database (25). S2 cells are a *Drosophila* cell culture system. Due to substantial structural homology between vertebrate and invertebrate integrins, as well as a similarity between many of the integrin-signaling pathways, information learned about integrin microclustering in *Drosophila* cells can be used to advance the understanding of vertebrate integrins (26).

The choice of *Drosophila* cell culture is optimal for these studies because rapid, simple, and selective reduction in protein expression is possible using RNAi (16, 27). A similar technique used in mammalian cell culture, short-interfering RNA (i.e., siRNA), often suffers from low specificity for the targeted protein and an immune response to the RNA. In RNAi experiments, approximately 500-bp double-stranded RNA corresponding to the mRNA sequence of the targeted protein is used to reduce protein expression. Whole-genome RNAi studies have been performed, and the sequences used to reduce protein expression in these studies are published and available in several online resources (28, 29). The RNAi

probes used in this study were selected from these resources. Two criteria were used in selecting the RNAi probes: thermodynamic binding efficiency and selectivity. The selectivity is a measure of other proteins that may be targeted by the RNAi probe. Since the goal of this work is to identify specific proteins that affect integrin microclustering, only probes with 100% selectivity to the targeted protein were chosen for the FRET studies (other targets, Table 1). The actin42A probe targets the entire class of actin proteins, but does not target other protein classes. Once internalized, the approximately 500- bp dsRNA is reduced to approximately 21-bp fragments.The thermodynamic binding efficiency presented in Table 1 is a measure of how many of the possible 21-mers have thermodynamically favorable binding to the target mRNA. This value is not necessarily reflective of the amount the

target protein's expression is reduced. For a given protein, RNAi probes with 100% selectivity and the highest efficiency were selected. Another important consideration is possible changes in cell viability after RNAi treatment. None of the RNAi treatments altered cell viability compared to cells that did not receive RNAi treatment (data not shown).

A cell line expressing green fluorescent protein (GFP) fused to actin 42A was used show that the RNAi protocol used in these studies facilitates the delivery of dsRNA into the cytoplasm. Four days after RNAi treatment against actin 42A, a 21% reduction in the GFP fluorescence was measured compared to cells that did not receive RNAi treatment (Supplemental Figure S2). The reduction in protein expression will vary with each RNAi probe. Typical RNAi knockdown efficiencies for *Drosophila* cell culture are between 95–99% and 62–100% using Western blotting and cell phenotype analysis, respectively (16, 30).

Cytoplasmic proteins that affect integrin microclustering

Figure 3 (black data bars) shows the average FRET values for at least 100 S2 cells expressing wild-type integrins and FRET reporters after the indicated RNAi treatment. The data were normalized and statistically compared to the value obtained for the no RNAi treatment data.

Four of the RNAi treatments resulted in higher levels of energy transfer compared to the no RNAi treatment data: vinculin, paxillin, rhea, and focal adhesion kinase. The higher energy transfer values indicate an increase in the microclustering of the FRET reporters, which may be due to integrin-specific interactions, non-integrin-specific interactions or a combination of both, as discussed above. This can be determined by measuring the energy transfer in a cell line expressing integrins and FRET control peptides (Fig. 3, gray data bars). If the increase in energy transfer measured after RNAi treatment for cells expressing integrins and FRET reporters is non-integrin-specific, then increased energy transfer is expected in the cell line expressing the FRET controls. However, if the increase in energy transfer is the result of integrin-specific interactions, no change in energy transfer is expected for the cell line expressing the FRET controls. There was no statistically significant change in energy transfer after any of the RNAi treatments for cells expressing the FRET controls. These results indicate that the increase in energy transfer measured in the cell line containing the FRET reporters, after vinculin, paxillin, rhea, and focal adhesion kinase RNAi treatment, is measuring integrin-dependent increases in FRET reporter microclustering. Reducing the expression of these cytoplasmic proteins increases FRET reporter clustering due to increased

integrin microclustering. These proteins prevent integrin microclustering under the conditions used in these studies.

It is not possible to relate the magnitude change in energy transfer to a magnitude change in integrin microclustering using Eq. 1. Furthermore, the change in integrin microclustering may be dependent on how much protein expression is reduced. For each RNAi-targeted protein, the amount its expression is reduced may differ. Different thermodynamic efficiencies (Table 1), the amount of target mRNA within the cell, and differential transport of the dsRNA probe across the cell membrane will influence how efficient the overall RNAi treatment is in reducing expression. The methodology reported here can be used to determine the cytoplasmic proteins that alter integrin microclustering, which has important implications for intracellular signaling events. On-going efforts will enable a quantitative connection between the change in energy transfer and the change in integrin microclustering.

Cytoplasmic proteins that affect the microclustering of integrin mutants

Details about the molecular mechanism of protein clustering can be obtained by studying protein mutants. Figure 4 (black data bars) shows the FRET values for S2 cells expressing αβV409D mutant integrins and FRET reporters after the indicated RNAi treatment. In addition to the four cytoplasmic proteins identified as increasing energy transfer in cells expressing wild-type integrins, an additional RNAi treatment show a statistically significant increase in energy transfer compared to wild-type cells. This protein is dreadlock,

which forms a link between integrins and receptor tyrosine kinases. This suggests that disruption of the cytoplasmic linkage between αβV409D integrins and receptor tyrosine kinases results in higher integrin microclustering.

A previous study revealed the microclustering of the αβV409D integrin mutant is dependent on the presence of other membrane proteins (6). When the extracellular domains of all membrane proteins were digested from the cell surface prior to expressing the integrins and FRET reporters, the microclustering of the αβV409D mutant decreased. In contrast, there was no change in the microclustering of wild-type integrins when the extracellular domains of other membrane proteins were removed from the cell membrane. The previous study did not reveal the identity of the membrane protein(s) responsible for the microclustering of the αβV409D mutant since all membrane proteins were simultaneously targeted for removal. In addition, the transmembrane and cytoplasmic domains of the other membrane proteins remained in the membrane, and key integrin contacts in the cytoplasm may not have been disrupted. The use of FRET reporters and RNAi, as outlined in this report, has the benefit over previous methods for measuring the molecular mechanism of receptor clustering because the entire protein is removed,not just a fragment of the protein, and an individual protein can be targeted. The FRET results for the αβV409D mutant reveal receptor tyrosine kinase is at least one membrane protein responsible for its altered microclustering, via the cytoplasmic protein dreadlock, compared to wild-type integrins.

In comparison to the αβV409D mutation, the αanaβ mutation's microclustering properties were altered only with RNAi treatment for paxillin at 3% to 5% ligand density (Fig. 4, gray data bars). When the same RNAi probe is used to reduce the expression of a

cytoplasmic protein in different populations of the same cell type (e.g. S2 cells), the magnitude of the change in energy transfer can be cautiously compared. The FRET data indicates a 1.6-fold increase in FRET after paxillin RNAi treatment as opposed to six- and four-fold increase with wild-type and αβV409D mutant integrins, respectively. The remaining RNAi treatments that were studied showed no statistically significant differences for the αanaβ mutation compared to the no RNAi treatment data. The lack of change in integrin microclustering for the αanaβ mutation reflects a 'defect' in the ability of the cytoplasmic proteins to participate in the microclustering of this mutation. The lack of change in energy transfer for the αanaβ mutation is not the result of higher microclustering levels prior to the RNAi treatments.The energy transfer value obtained for the αanaβ no RNAi treatment data is similar to the values for cells expressing wild-type and the αβV409D mutation (Table 2). Therefore, αanaβ integrin microclustering levels are similar to other cell lines at 3% to 5% ligand density, prior to RNAi treatment. Additionally, higher energy transfer values have been measured for this cell line in the presence of a high ligand concentration (6), indicating that increased microclustering is possible under some circumstances.

It should not be surprising that decreased energy transfer was not measured after any of the RNAi treatments. As discussed above, at 3% to 5% ligand density the energy transfer measured before treatment is from non-integrin-specific microclustering of the FRET reporters, and the integrin-specific microclustering that may be present is below the detection limit for this assay. The cytoplasmic proteins that prevent integrin microclustering, in the absence of binding to extracellular ligand, have been identified. When the expression of these

proteins is reduced, increased energy transfer is measured. When the ligand density is 50% on the glass surface, integrin microclustering levels are higher than what is measured at 3% to 5% ligand densities. Preliminary studies utilizing cells spread on a densely coated ligand surface have revealed that decreased energy transfer values after RNAi treatment can be obtained (unpublished data).

CONCLUSION

The organization of the cell membrane is important for many basic cell functions, and can lead to pathological conditions when it is altered. Currently, few non-invasive analytical techniques can measure intracellular events that lead to changes in the organization of the cell membrane. The combination of FRET and RNAi has the unique capacity for measuring integrin organization without altering the integrin dynamics. Specific cytoplasmic events leading to integrin microclustering can be identified. When cells are spread on a surface with 3% to 5% ligand density, it was found that four proteins that connect integrins to the cytoskeleton also affect integrin microclustering. The molecular mechanism of integrin microclustering is further understood by analyzing integrin mutants. The microclustering of a mutation (αβV409D) that affects the ligand-binding domain is more sensitive to cytoplasmic interactions that indirectly link integrins to receptor tyrosine kinases compared to wild-type integrins. On 3% to 5% ligand surface densities, an alpha cytoplasmic mutation (αanaβ) loses its sensitivity to microclustering when the expression of all cytoplasmic proteins studied, except paxillin, is reduced. This methodology is not limited to integrins. Similar strategies

can be used to study other classes of cell membrane receptors, and will enable a complete understanding of how receptor organization is directed by cytoplasmic binding events.

ACKNOWLEDGMENTS

This work was supported by the Roy J. Carver Charitable Trust (Muscatine IA), National Science Foundation (CHE-0845236) and Iowa State University Office of the Vice President for Research. The authors thank Roger Tsien (Howard Hughes Medical Institute, La Jolla, CA) for the original mCherry plasmid, Atsushi Miyawaki (Riken, Wako-city, Saitama, Japan) for the original Venus plasmid, Man-Yu Yum (Iowa State University) for help with the statistical analysis, Saiju Mathew (Iowa State University) for developing the FRET ImageJ plug-in, and Dilshan Shanaka Harischandra (Iowa State University) for synthesizing the RNA.

REFERENCES

1. Giancotti FG, and Ruoslahti E (1999) Science 285:1028

2. Phizicky EM, and Fields S (1995) Microbiol Rev 59:94

3. Selvin PR (2000) Nat Struct Biol 7:730

4. Buensuceso C, de Virgilio M, and Shattil SJ (2003) J Biol Chem 278:15217

5. Kim M, Carman CV, Yang W, Salas A, and Springer TA (2004) J Cell Biol 167:1241

6. Smith EA, Bunch TA, and Brower DL (2007) Anal Chem 79:3142

7. Ginsberg MH, Partridge A, and Shattil SJ (2005) Current opinion in cell biology 17:509

8. Martin-Bermudo MD, and Brown NH (1996) J Cell Biol 134:217

9. Helsten TL, Bunch TA, Kato H, Yamanouchi J, Choi SH, Jannuzi AL, Feral CC, Ginsberg MH, Brower DL, and Shattil SJ (2008) Mol Biol Cell 19:3589

10. Subauste MC, Pertz O, Adamson ED, Turner CE, Junger S, and Hahn KM (2004) J Cell Biol 165:371

11. Legate KR, Montanez E, Kudlacek O, and Fassler R (2006) Nat Rev Mol Cell Biol 7:20

12. Vicente-Manzanares M, Choi CK, and Horwitz AR (2009) J Cell Sci 122:199

13. Bunch TA, and Brower DL (1992) Development 116:239

14. Bunch TA, Grinblat Y, and Goldstein LS (1988) Nucleic Acids Res 16:1043

15. Jannuzi AL, Bunch TA, Brabant MC, Miller SW, Mukai L, Zavortink M, and Brower DL (2002) Mol Biol Cell 13:1352

16. Clemens JC, Worby CA, Simonson-Leff N, Muda M, Maehama T, Hemmings BA, and Dixon JE (2000) Proc Natl Acad Sci U S A 97:6499

17. March JC, and Bentley WE (2006) Biotechnol Bioeng 95:645

18. Chen H, Puhl HL, 3rd, Koushik SV, Vogel SS, and Ikeda SR (2006) Biophysical journal 91:L39

19. Xia Z, and Liu Y (2001) Biophysical journal 81:2395

20. Zal T, and Gascoigne NR (2004) Biophysical journal 86:3923

21. Zar J (1999) Biostatistical Analysis. Prentice Hall, Upper Saddle, NJ

22. Fogerty FJ, Fessler LI, Bunch TA, Yaron Y, Parker CG, Nelson RE, Brower DL, Gullberg D, and Fessler JH (1994) Development 120:1747

23. Bunch TA, Helsten TL, Kendall TL, Shirahatti N, Mahadevan D, Shattil SJ, and Brower DL (2006) J Biol Chem 281:5050

24. FLIGHT [http://flight.licr.org/]

25. PeptideAtlas [www.mop.unizh.ch/peptideatlas]

26. Brower DL (2003) Current opinion in cell biology 15:607

27. Armknecht S, Boutros M, Kiger A, Nybakken K, Mathey-Prevot B, and Perrimon N (2005) Methods Enzymol 392:55

28. FlyBase. (http://flybase.bio.indiana.edu).

29. Heidelberg [http://www.dkfz.de/signaling2/rnai/ernai_probes.php]

30. Kiger AA, Baum B, Jones S, Jones MR, Coulson A, Echeverri C, and Perrimon N (2003) J Biol 2:27

Table 1 RNAi probes used to reduce protein expression in S2 cells

Cytoplasmic Protein	RNAi probe ID	Thermodynamic binding efficiency[a]	Other protein targets
Vinculin (Vin)	HFA18728	33/493	No
Paxillin (Pax)	BKN29242	72/293	No
Rhea	HFA11300	101/487	No
Focal Adhesion Kinase (FAK)	HFA07426	136/483	No
Integrin Linked Kinase (ILK)	HFA11868	89/469	No
Dreadlock (Dock)	HFA00812	44/220	No
Steamer Duck (SD)	HFA17070	19/249	No
Actin42A	HFA04835	53/480	Yes

The RNAi probe ID, efficiency and other target values are from published and online resources: http://flyrnai.org

[a] The first value in the column is the number of 21 base pair oligonucleotides that have thermodynamically favorable binding to the target mRNA,and the second value in the column is the total number of 21 base pair oligonucleotides generated from the RNAi probe

Table 2 Mean FRET values from at least 100 cells expressing FRET reporters or controls and the indicated integrins: αβ, wild-type; αanaβ, α cytoplasmic mutation; αβV409D, β extracellular domain mutation

αβ FRET Reporters	**αanaβ FRET Reporters**	**αβV409D FRET Reporters**	**αβ FRET Controls**
0.013	0.016 (p=0.33)	0.017 (p=0.23)	0.013 (p=0.96)

Cells are spread on a glass surface coated with a 3% to 5% ligand density, all data are statistically compared to the value obtained for cells expressing wild-type integrins with FRET reporters

Fig. 1 Schematic showing FRET assay and proteins known to be involved in integrin-signaling complexes. Cytoplasmic proteins targeted in this study to measure how they affect integrin micro-clustering: rhea, vinculin, actin, integrin-linked kinase (ILK); CG32528, paxillin, dreadlock (Dock); steamer duck and focal adhesion kinase (FAK). (top) No energy transfer takes place when FRET reporters are separated by greater than 10 nm. (bottom) Reduced expression of a target cytoplasmic protein (e.g., Paxillin) increases integrin clustering and increases energy transfer from donor (D) fluorescent protein to acceptor (A) fluorescent protein. This is a static picture of a dynamic system.

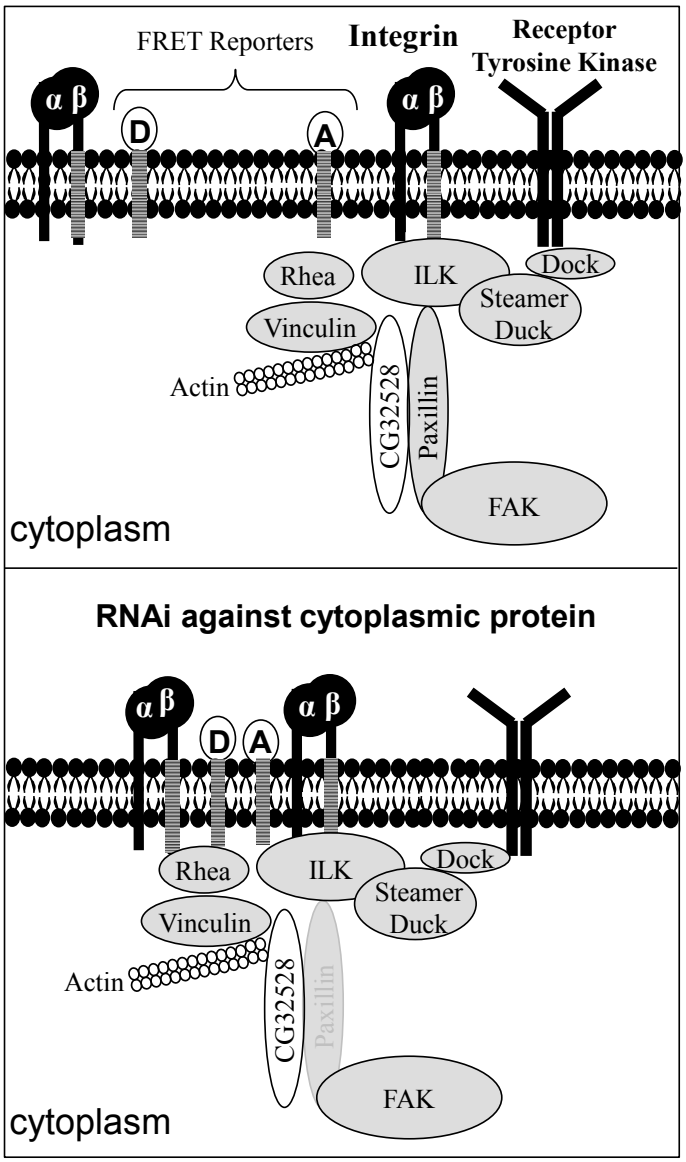

Fig. 2 Fluorescence images of a transformed Drosophila S2 cell, expressing αPS2CβPS integrins and FRET reporters. Image obtained using (top) donor filter set; (middle) acceptor filter set; (bottom) FRET filter set. Color has been added to correspond to the emission filter used to generate each image. FRET values are calculated on a pixel-by-pixel basis according to Eq. 1. A region of interest is generated for each cell that excludes fluorescence emanating from inside the cell. An example region of interest is shown in the top image (green)

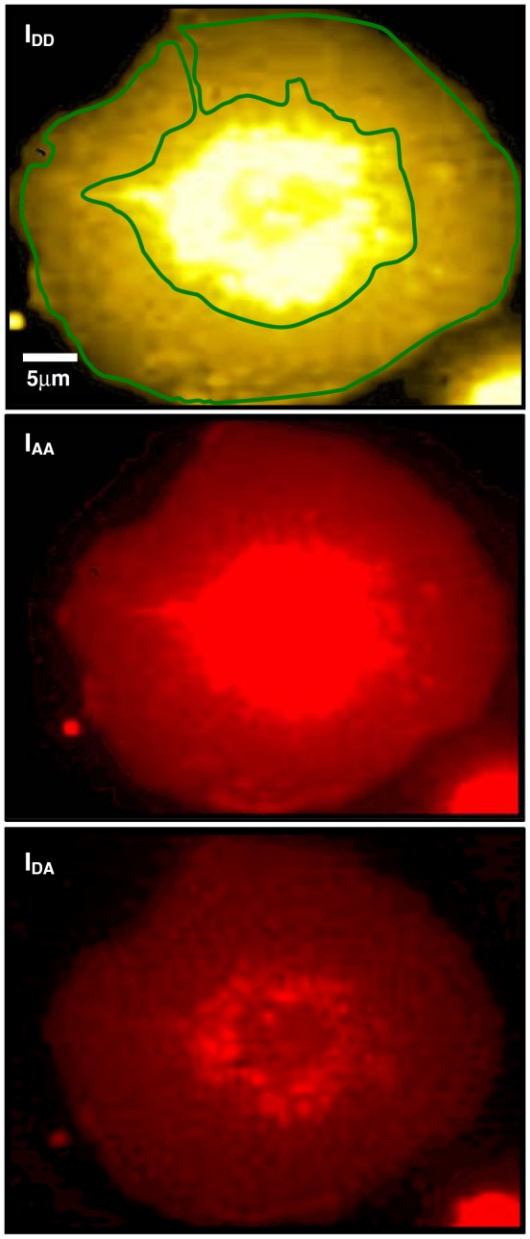

Fig. 3 Normalized FRET values for S2 cells expressing wild-type integrins and FRET reporters (black data bars) or wild-type integrins and FRET controls (gray data bars) after the indicated RNAi treatment. All values are normalized to the no RNAi treatment data (Table 2). A p value below 0.05, shows statistical evidence that the energy transfer measured after RNAi treatment is altered compared to the no RNAi treatment data set. The abbreviations used in this figure are listed in Table 1

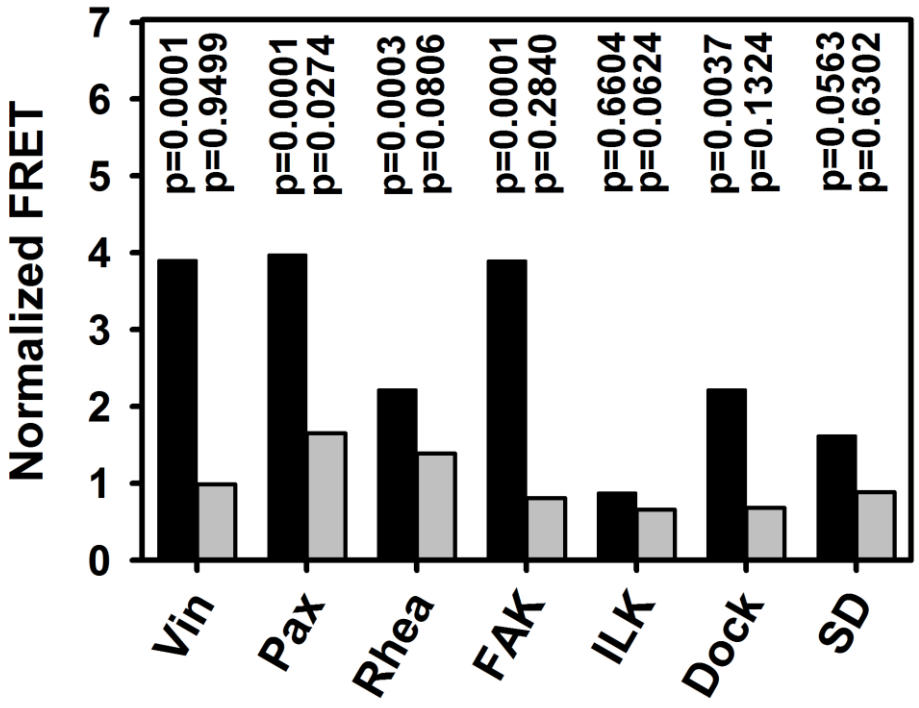

Fig. 4 Normalized FRET values for S2 cells expressing αβV409D mutant integrins and FRET reporters (black data bars) or αanaβ mutant integrins and FRET reporters (gray data bars) after the indicated RNAi treatment. A p value below 0.05 shows statistical evidence that the energy transfer measured after RNAi treatment is altered compare to the no RNAi treatment data set. The abbreviations used in this figure are listed in Table 1

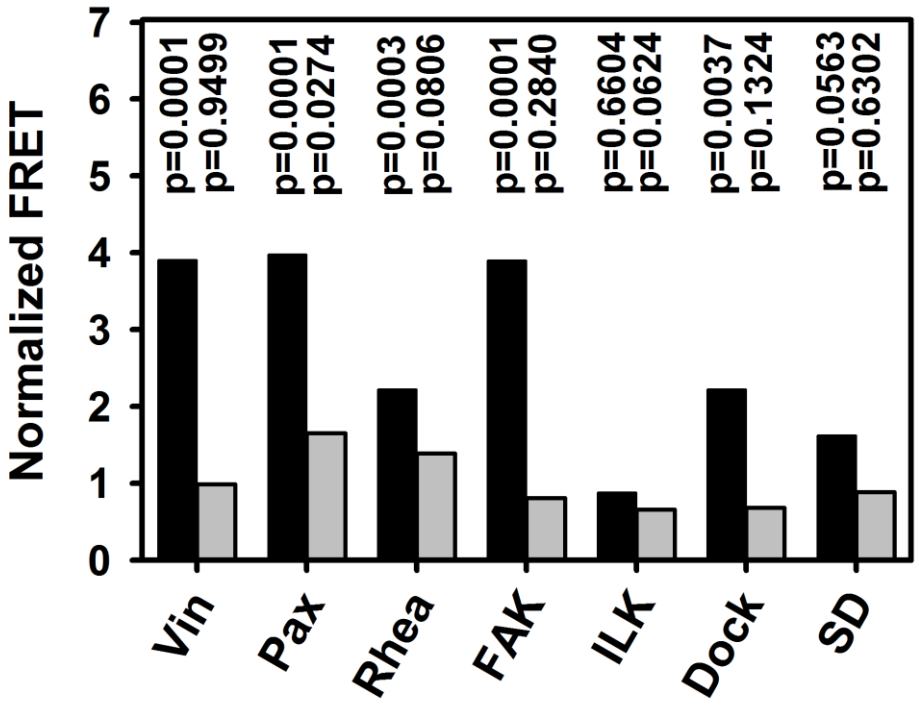

Supplemental Experimental Methods

FRET Bleed-through Factors

The factors *a*, *b*, *c*, and *d* account for bleed-through of: acceptor into the FRET filters, acceptor into the donor filters, donor into the acceptor filters, and donor into the FRET filters, respectively. These values were measured in cell lines that contained only the acceptor FRET control plus wild-type integrins (for a and b) or donor FRET control plus wild-type integrins (for c and d). The data (not shown) for these bleed-through factors reveal a dependence on the amount of donor and acceptor expressed in the cell, and were fit to exponential curves:

$$a = 0.103 + 0.565 \cdot \exp(-0.540 \times 10^{-2} \cdot I_{AA}); \quad (2)$$

$$b = 0.013 + 0.274 \cdot \exp(-0.466 \times 10^{-2} \cdot I_{AA}); \quad (3)$$

$$c = 0.077 + 0.344 \cdot \exp(-0.905 \times 10^{-2} \cdot I_{DD}); \quad (4)$$

$$d = 0.276 - 0.027 \cdot \exp(-0.346 \times 10^{-3} \cdot I_{DD}). \quad (5)$$

For the FRET calculations, if the donor fluorescence intensity was below 50 or the acceptor fluorescence intensity was below 50, the cell was rejected from the analysis. These lower threshold values were used to minimize the residual between the exponential fit and experimental bleed-through factor experimental data. The applied bleed-through factor was determined on a pixel-by-pixel basis during the FRET calculation. Background subtraction was performed on all images using an average intensity from cell-free regions of the image, and zero cellular autofluorescence was observed in the donor, acceptor or FRET images using the stated acquisition parameters.

Preparation of RBB-Tiggrin Surfaces

RBB-tiggrin is a bacterial fusion protein containing the integrin binding domain of the extracellular matrix protein tiggrin. RBB-tiggrin was produced as described previously.[17] Glass microscope slides (Fisherbrand, Fisher Scientific) were sterilized in 70% ethanol for 15 min and dried in a sterile environment. They were coated with a sterile solution containing 0.05 μg/mL RBB-tiggrin in pH 7 phosphate-buffered saline (PBS) for 2 h. The RBB- tiggrin solution was then removed and any remaining exposed glass surface was blocked using a 10 mg/mL solution of bovine serum albumin in pH 7 PBS. Coated slides were stored overnight at 2 °C and used within 24 h.

Actin-GFP Assay

S2 cells expressing integrins, UASpGFP tagged actin42A and pAdhGAL4, were RNAi treated for actin42A. Using these constructs, expression of actin42A-GFP is constitutively active. After RNAi treatment and incubation for 4 days, cells were transferred from the cell culture dish and collected by centrifugation. Cells were prepared for microscopy as described above for the FRET assay. The cells were imaged using a GFP filter set (excitation 470/50 nm and emission 545/75 nm).

Figure S1: Distribution of FRET values for one cell**.** The X-axis represents FRET value and the Y-axis denotes the number of pixels with a given FRET value. All values reported in this image are multiplied by a factor of 100, relative to the FRET values reported in Table 2 of the main text.

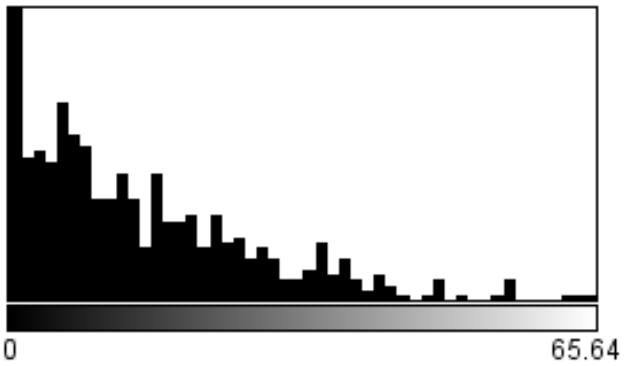

Figure S2: RNA knock-down efficiency. In order to estimate the efficacy of the RNAi treatments in reducing protein expression, a cell line expressing cytoskeletal protein actin42A tagged with green fluorescent protein (GFP) was utilized. The cells were treated with dsRNA for actin42A. This dsRNA also targeted five other actins expressed in S2 cells. Fluorescence intensities were measured after incubating 4 days with dsRNA. Shown in Figure S2A (left) is the fluorescence image of control cells expressing actin42A-GFP and (right) the fluorescence image of the same cell line after actin42A RNAi treatment. Both images are shown in the same intensity scale. The histograms in Figure S2B show the fluorescence of 100 cells (left) for control cells expressing actin42A-GFP and (right) the same cell line after actin42A-average. The mean fluorescence value for the control cell line is 590 and after RNAi treatment the mean value is 466. A statistically significant reduction in fluorescence is measured after RNAi treatment, as determined using the Welch Test (p=0.008).

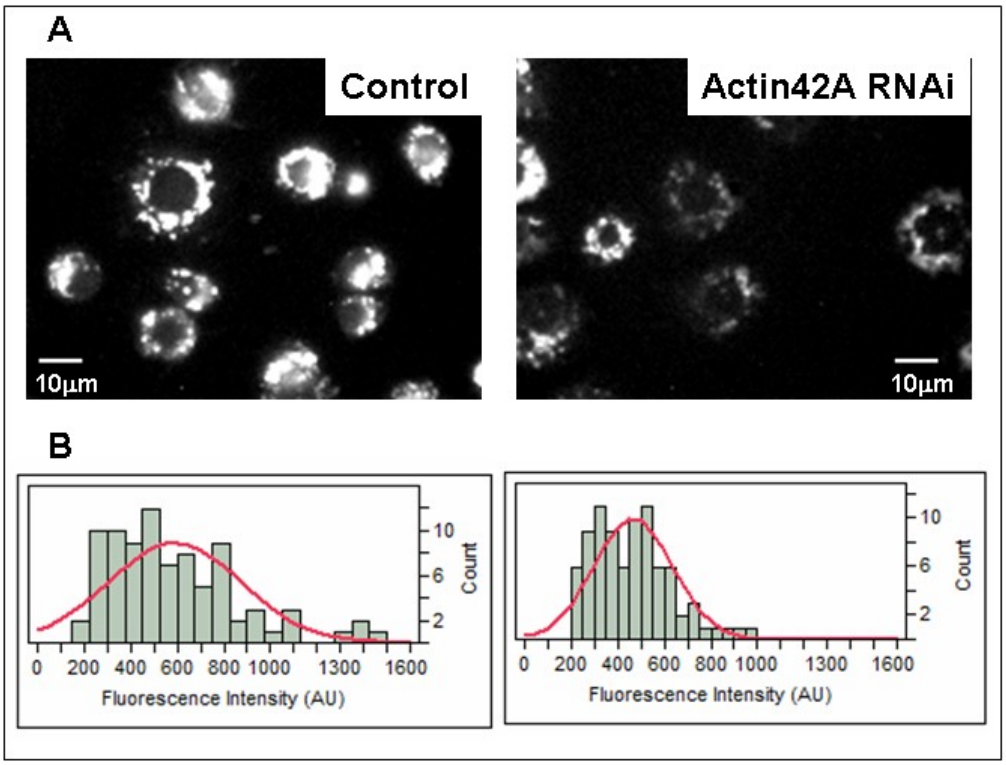

CHAPTER 3: NON-INVASIVE MEASUREMENTS OF CHOLESTEROL'S ROLE IN INTEGRIN MICROCLUSTERING

A paper submitted to Biophysical Journal

Deepak Dibya and Emily A. Smith

ABSTRACT

Reported herein is a method to study the role of cholesterol in the microclustering of a ubiquitous class of membrane receptors termed integrins. Integrin microclustering was measured using a fluorescence resonance energy transfer (FRET) assay that does not require the direct attachment of fluorescent donors or acceptors onto the integrins; thus minimizing unwanted perturbations to integrin clustering. Membrane cholesterol levels were reduced using methyl-β-cyclodextrin (mβCD), as confirmed using Amplex red assays. Subsequent changes in integrin microclustering were measured in cells expressing wild-type or mutant integrins. Changes in energy transfer after reducing cholesterol concentrations provided evidence for the role of cholesterol in integrin microclustering. Restoration of original cholesterol levels was used to confirm that the measured changes in membrane properties were cholesterol-dependent. While less integrin microclustering was measured after

cholesterol depletion for a cell line expressing wild-type integrins, there was no change or a significant increase in integrin microclustering after cholesterol depletion for cells expressing cytoplasmic or ligand-binding domain integrin mutants, respectively. Possible correlations between lipid diffusion and integrin microclustering were studied with fluorescence recovery after photobleaching (FRAP) using a fluorescent lipid mimetic. Similar lipid diffusion coefficients were measured irrespective of the integrins being expressed before and after cholesterol depletion.

INTRODUCTION

Survival, growth, proliferation, differentiation and proper functioning of cells are largely dependent on maintaining a dynamic flow of information between the external and internal environments of the cell (1). Towards this end, cells employ receptors to relay information inside and outside of the cell (2-5). One of the mechanisms for signal transduction involves clustering of receptors within the cell membrane. Receptor clustering has been involved in many vital processes such as immunological synapse formation, actin cytoskeleton regulation and leukocyte regulation (6-8). A class of receptors that are fundamental to many critical cellular functions is integrins (1, 9). They are heterodimeric proteins composed of one α subunit noncovalently associated with one β subunit. They mediate signaling through the cytoplasm by binding to adapter proteins and through the extracellular matrix by binding ligand (9, 10).

Fluorescence microscopy has been used to study the clustering of integrins within the cell membrane (11-13). Observing clusters in live cells that are smaller in size than the diffraction-limit of light requires an imaging technique such as FRET (14-16). In previous studies, integrin microclustering was measured using a FRET assay that did not require attaching donor and acceptor FRET pairs directly to the integrins (17, 18). Energy transfer was measured using reporter peptides, which were generated by cloning the FRET donor or acceptor fluorescent protein to the transmembrane and cytoplasmic domain of the integrin β subunit. Hereafter, these will be referred to as FRET reporters. The FRET reporters were co-expressed with unaltered integrins (17, 18). When integrins cluster in the membrane, so do the FRET reporters. This decreases the average separation distance between the donor and acceptor FRET reporters, and an increase in energy transfer is measured. Conversely, when the separation distance between integrins increases, less energy transfer is measured using the FRET reporters. Control experiments showed that the FRET reporters did not alter key integrin properties, and energy transfer was not measured when the FRET reporters are expressed but integrins are not.

In this report, the effect of cholesterol on the microclustering of αPS2CβPS integrins is measured using the above mentioned FRET assay. Cholesterol is a small lipid molecule that intercalates between the fatty acyl chains of the lipid bilayer. It is known to maintain membrane structure, regulate membrane fluidity and directly interacts with some membrane proteins (19-23). Cholesterol is an important constituent in membrane nanodomains (i.e., lipid rafts), areas with non-uniform compositions of lipids and proteins relative to the bulk membrane. Membrane nanodomains have been shown to play a role in many signal

transduction events, such as immunoglobulin E (IgE) signaling during the allergic immune response, T-cell activation, glial-cell-derived neurotrophic factor signaling and integrin leukocyte function-associated antigen-1-mediated cell binding (24-28).

Cholesterol levels can be modulated in the cell membrane using cyclodextrins, which partition cholesterol from cellular membranes into their interior pore. Cyclodextrins can also partition other membrane components, but preferentially extracts cholesterol over other lipid components (29). Herein, cholesterol extraction is combined with the previously mentioned FRET assay in order to measure the role of cholesterol in integrin microclustering. In combination, alterations in lipid diffusion were observed in live cells using fluorescence recovery after photobleaching (FRAP) under reduced cholesterol levels.

MATERIALS AND METHODS

S2 cell culture

All experiments were performed using transformed *Drosophila* S2 cells. Cells were cultured in Shields and Sang M3 insect medium (M3, Sigma) with heat-inactivated 10% fetal bovine serum (Irvine Scientific), 12.5 mM streptomycin, 36.5 mM penicillin, and 0.2 μM methotrexate (Fisher Scientific) in a 22 °C incubator. For FRET assays, cells were co-transfected to express α and β integrin subunits and FRET reporters. Complete protein sequences for the FRET reporters containing mVenus and mCherry fluorescent proteins, and mutant integrin subunits have been published previously (17, 30-32). For FRAP assays, cells

were transfected to express integrin subunits (i.e., no FRET reporters). All the exogenous proteins contain the heat shock promoter.

Cholesterol depletion, restoration and addition

For cholesterol depletion, the cells were centrifuged at approximately 600×g and the resulting pellet was resuspended at a concentration of 2×10^6 cells/mL in serum-free M3 medium containing 0.25% methyl-β-cyclodextrin (mβCD) (Sigma-Aldrich, St. Louis, MO) and incubated at 22 °C for 30 minutes. For cholesterol restoration, cholesterol depleted cells were washed with serum free medium and then resuspended in M3 medium containing 100μM cholesterol loaded cyclodextrin (chol-mβCD) complex (Cyclodextrin Technologies Development, High Springs, FL) for 1 hour at 22 °C.

For cholesterol addition to untreated cells, the cells were centrifuged at approximately 600×g, and were resuspended in M3 medium containing four different concentrations (100μM, 250μM, 500μM and 1000μM) of chol-mβCD for 1 hour at 22 °C. Prior to FRET, FRAP or Amplex Red analyses, the cholesterol depleted, restored or added cells were washed in serum free medium to remove the cyclodextrin.

Quantitative measurements of cholesterol

The total lipid content of cells was extracted using the Bligh–Dyer method (33). Briefly, 3.0 mL chloroform/methanol (2:1 v/v) was added to 1.0 mL of ~ 10^6 cells followed

by vigorous vortexing for 15 minutes. Then, 1.0 mL of 1.0 M NaCl was added to the solution and the sample was vortexed for 1 minute. The solution was allowed to sit for 10 minutes and the chloroform phase was collected and filtered using Whatman filter paper no. 1. The chloroform was evaporated under nitrogen, and the cellular lipids were resuspended in phosphate buffer containing 0.1 M potassium phosphate, pH 7.4, 50 mM NaCl, 5 mM cholic acid, and 0.1% Triton X-100.

Cholesterol levels were quantified using an Amplex Red Cholesterol Assay (Life Technologies, CA) without cholesterol esterase (34). Cholesterol in the lipid extracts was oxidized by cholesterol oxidase to produce H_2O_2. In the presence of horseradish peroxidase, the non-fluorescent 10-acetyl-3,7-dihydoxyphenoxazine (Amplex Red) reacts with H_2O_2 with 1:1 stoichiometry to produce a highly fluorescent species, resorufin. Fluorescence was measured with a microplate reader (Synergy HT fluorescent platereader, BioTek, CA) using the excitation filter 530/25 nm and emission filter 590/35 nm. The cholesterol concentration was calculated using the equation for a best fit line to a calibration curve (Supplementary Figure S2).

FRET and FRAP assay

Cells were transferred from the cell culture dish to a polypropylene tube and heat-shocked for 30 min at 36°C to induce the expression of integrins and FRET reporters. To achieve maximum protein expression, cells were then placed in a 22°C incubator for 3 hrs. After incubation, the cells were subjected to cholesterol depletion/restoration as mentioned

above. The cell counts were adjusted to 5×10^5 cells/mL prior to placing them on a ligand-coated substrate, the preparation of which has been described previously (18). The cells were allowed to spread onto the ligand coated substrate for 1 hour, followed by FRET data collection within the next hour, as described in previously (17, 18).

For FRAP measurements, a carbocyanine DiD dye (Life Technologies, CA) was added to the untreated, cholesterol depleted or restored cells at a final concentration of 11.85 μM. The cells were immediately plated onto the ligand coated substrate. Cells were allowed to spread in the dark for 1 hour. The medium was then replaced with 20 mM BES Tyrodes buffer prior to FRAP analysis.

The microscope used for these studies contains two excitation light paths: one for a 635 nm diode laser (Newport Corp.) and a second for a mercury (Hg) lamp. The Hg lamp was used to image the cells before and after photobleaching the membrane incorporated DiD dye with the laser that was focused to a 3.14 μm ($1/e^2$) diameter spot. A laser shutter and CCD (Acton Photon Max 512, Princeton) shutter were synchronized with an external trigger. The trigger timing was: 0.45 seconds between image capture, 0.35 second for image capture, and 0.35 second for the photobleaching laser pulse. The diffusion coefficients were calculated as previously reported (35). Each reported diffusion coefficient represents an average of 10 measurements on different cells. Statistical significance was assessed using the student *t*-tests with 95% significance to compare the depleted/restored data set to the untreated data set.

Data Analysis - FRET

The FRET data were analyzed using an in-house developed Java plug-in for the software ImageJ. After subtracting the background value from each pixel, the plug-in calculates a FRET (E_{app}) value on a pixel-by-pixel basis using equation 1 (36):

$$E_{app} = \frac{I_{DA} - (a - bd)I_{AA} - (d - ac)I_{DD}}{I_{DA} - (a - bd)I_{AA} - (d - ac - G)I_{DD}} \qquad (1)$$

where I_{DA}, I_{AA}, and I_{DD} are intensities obtained from the images with the FRET, acceptor, and donor filters, respectively. The terms a, b, c and d account for the bleedthrough in the filter sets as previously described (17, 18). The G term in equation 1 is instrument specific and correlates to the decrease in donor fluorescence with an increase in acceptor fluorescence due to energy transfer (37). The G value for the instrument set up used in these studies is 1.419.

Each FRET value represents 100 independent measurements from 3 replicate experiments. Only membrane regions (i.e., excluding regions of the cell where intracellular FRET reporters contribute to the signal) are included in the measurement. All FRET data were statistically analyzed using the software JMP 7 (SAS Institute Inc, Cary, USA) with statistical consulting from Iowa State University Department of Statistics. The raw FRET data, being not normally distributed was log transformed and the means were calculated (38, 39). The means of the log transformed data were compared between FRET data sets of treated and untreated cells. After confirming the unequal variance among the data sets, statistical significance between the data sets was assessed using Welch *t*-tests. The significance of the statistical test is indicated by p-values. A statistically significant p-value is

one that is below 5%, indicating that the means from the two data sets are not the same. A p-value higher than 5% indicates that there is not enough statistical evidence to show dissimilarity between the two data sets. The data is reported in the original data scale by converting the means of the transformed data as discussed in standard statistics text books (40).

RESULTS AND DISCUSSION

A schematic of the assay used to measure changes in integrin microclustering due to altered cholesterol levels is shown in Figure 1. When the separation distance between integrins decreases, the separation distance between the donor and acceptor FRET peptides decreases, as has been previously reported (17). This results in more energy transfer between the donor and acceptor fluorescent proteins. Similarly, less energy transfer is measured when the integrin separation increases, since the separation distance between FRET reporters also increases. The mechanism of the co-clustering of integrins and FRET reporters is currently unknown. However, the β transmembrane and cytoplasmic domains contained in the FRET reporters have been shown to meet the minimum requirement for clustering with integrins *in vivo* (41).

The cell line utilized for these studies is *Drosophila* S2 cells expressing αPS2CβPS integrins due to the wealth of data available on the microclustering of this integrin (17, 18). This enables a direct comparison to the data obtained for the microclustering of this integrin upon altering cholesterol levels. There is substantial structural homology between vertebrate

and invertebrate integrins, and many similarities between the integrin-signaling pathways (42). The information learned about integrin microclustering in S2 cells can be used to advance the understanding of vertebrate integrins. Similar methodology as reported here can also be developed for vertebrate cell culture system.

Unlike mammalian cells, *Drosophila* cells are sterol auxotrophs and derive sterols from their environment (43, 44). In the case of cultured *Drosophila* cells, the source of sterols is from the fetal calf serum added to the growth medium. As confirmed by reverse phase high-performance liquid chromatography, the main sterol incorporated in the cell membrane of the cultured cells is cholesterol (Supplementary Figure 1).

Figure 2 shows the developed strategy to measure the role of cholesterol in integrin microclustering. Cholesterol concentrations, lipid diffusion coefficients, and integrin microclustering levels were measured in three cell populations: untreated cells containing native levels of cholesterol; cells with depleted levels of cholesterol; and cells first depleted of cholesterol and then restored to native levels. Comparison of the measured parameters in the three populations provides evidence for the role of cholesterol in altering the organization of integrins in the cell membrane.

Prior to measuring integrin microclustering and lipid diffusion, cholesterol levels were quantified in the three cell populations. Figure 3 (black data bars) shows the average cholesterol concentration per cell prior to cholesterol depletion. The cells utilized in these studies expressed wild-type or mutant integrins and FRET reporter peptides. Two well-characterized integrin mutants have been used in this study. The mutant αanaβ integrin contains a two-point mutation in the α subunit near a site where cytoplasmic proteins are

known to bind and is considered to mimic the signal transduction from inside to outside the cell (45). The mutant αβV409D integrin contains a single point mutation located in the extracellular domain of the β subunit and is considered to mimic signal transduction from outside to inside the cell (45). Compared to the wild-type integrins, increased affinity for ligand has been observed with both mutants (17).

As shown in Figure 3, there are only slight variations in cholesterol levels in untreated cells (black data bars). This is consistent with all three cells lines having been derived from the same S2 parent cell line, and with previous studies where 10^{-14} to 10^{-16} moles cholesterol/cell has been measured (46, 47). Regardless of the starting cholesterol concentration, there is an approximately 50% reduction in cholesterol concentration in all cells lines after treatment with mβCD (white data bars) relative to untreated cells.

The measured reduction in cholesterol after mβCD treatment is primarily from loss of cholesterol in the cell membrane, and not the loss in the intracellular cholesterol. This is important to consider since the aim of this work is to measure the role of cell membrane cholesterol on integrin microclustering. The individual contributions from intracellular cholesterol and plasma membrane cholesterol cannot be established by the Amplex red assay since total cellular cholesterol is measured. In order to minimize the contribution of intracellular components in the Amplex red assays, no cholesterol esterase was used. This ensures that intracellular cholesterol esters do not contribute to the measurement. In a recent study, a direct *in-situ* analysis of plasma membrane cholesterol levels using a fluorescent probe showed ~ 70% decrease in membrane cholesterol compared to the control cells that did not undergo cyclodextrin treatment (48). Since the plasma membrane is the only cell surface

in direct contact with mβCD, only plasma membrane cholesterol is available for partitioning into the mβCD. The measured 50% reduction in cholesterol levels is within the 20-80% range that has been measured in previous studies using cyclodextrins (47, 49-51).

In addition to reducing cholesterol concentrations, it was hypothesized that further information about the role of cholesterol in integrin microclustering could be obtained by increasing the concentration of cholesterol in the membrane. Considering the cell density used in these studies, the native cholesterol concentration is ~ 4 μM. The concentration of cholesterol in the M3 medium supplemented with 10% fetal bovine serum is ~ 45 μM. In addition to this basal cholesterol concentration, an additional 100, 250, 500 or 1000 μM of chol-mβCD was added to the growth medium. Figure 4 shows the average cholesterol concentration in cells that were treated with additional cholesterol did not result in a statistically significant increase in membrane incorporated cholesterol. The results indicate that the level of cholesterol in the untreated membrane is saturating under these conditions, and further increase in membrane cholesterol using this methodology is not possible.

Cholesterol affects lipid diffusion

Cholesterol has been shown to affect lipid diffusion in the cell membrane (50, 52, 53). To evaluate the role of cholesterol in lipid diffusion in wild-type and mutant integrin expressing S2 cells, FRAP measurements were performed to measure the diffusion coefficient of a fluorescent lipid analog: DiD. FRAP involves photobleaching DiD in a defined area in the cell membrane, and then recording the time it takes to repopulate the

photobleached species by the diffusion of the unbleached dye molecules. To avoid any spectral interference due to the fluorescence from the FRET reporters, cells expressing wild-type or mutant integrins with no FRET reporter were used for the FRAP studies. Supplementary Figure S3 shows a representative FRAP recovery curve used to measure the DiD diffusion coefficients (35).

Table 1 shows the diffusion coefficients measured for the three cell lines before and after cholesterol depletion. Across the three cell lines, the results indicate a similar level of membrane fluidity in untreated cells, as measured by DiD diffusion. These diffusion coefficients are consistent with the values obtained in other cell types, which range from 10^{-9} – 10^{-10} cm^2/s (50, 52-54). When cholesterol levels were depleted to 50% of the starting concentration, membrane fluidity increased in all the three cell lines by approximately 20 to 40%. This result was found to be a statistically significant increase relative to the values obtained prior to cholesterol depletion, and is consistent with previous results (50).

Cholesterol affects integrin microclustering

Cells were spread on a glass substrate coated with a ligand for the αPS2CβPS integrins at a ligand surface density of 3% to 5%. In order to ensure integrin-ligand interactions were the only mechanism for cell spreading, non-specific interactions with the glass substrate were inhibited by coating the remaining exposed glass with bovine serum albumin. Previous studies have found that the properties of integrin microclustering are dependent on the ligand's surface density (17, 18). Under these conditions, the role of

cholesterol in integrin microclustering with minimal binding to extracellular ligand is being measured. Similar studies could be performed at higher ligand densities.

Table 2 shows the average FRET values for the three cell lines before and after cholesterol depletion. At 3% to 5% ligand surface density, the mean FRET value for cells expressing wild-type or mutant integrins and FRET reporters indicates statistically similar levels of energy transfer for all three cells lines (untreated cells). These results indicate similar amounts of integrin microclustering in all cell lines before cholesterol depletion, and are consistent with previous studies (18).

After reducing membrane cholesterol concentrations by 50%, integrin microclustering is altered in two of the three cell lines studied (Table 2, Cholesterol depleted cells). There is a 50% decrease in energy transfer for cells expressing wild-type integrins after cholesterol reduction, indicating that there is less microclustering of αPS2βPS integrins. For cells expressing αanaβ integrins, there was no statistically significant change in energy transfer after cholesterol depletion. There is a more than 3-fold increase in energy transfer for the cells expressing αβV409D mutant integrins after cholesterol depletion. The increase in energy transfer indicates that cholesterol depletion allows the αβV409D integrins to reduce their separation distance when there is less cholesterol in the membrane.

The energy transfer measured using the FRET assay depicted in Figure 1 is a result of both integrin-specific interactions with the FRET reporters and non-integrin specific interactions from many possible sources. Assuming the non-integrin specific contributions to energy transfer are similar for the three cells lines derived from the S2 parent cell line, the differences in energy transfer listed in Table 2 are primarily from integrin-specific

interactions with the FRET reporters. The lipid diffusion coefficients measured after cholesterol depletion support this assumption. There is an increase in the lipid diffusion coefficient after cholesterol depletion for all three cell lines (Table 1), which could result in an increase in transient interactions between donor and acceptor FRET reporters during the multi-second acquisition times used to collect the FRET data. However, there is an increase in energy transfer only for the cholesterol depleted cells expressing αβV409D integrins.

The changes in energy transfer measured after cholesterol depletion report on the amount of integrin microclusters that are cholesterol dependent. There may be integrin microclusters present that are not altered by reducing cholesterol concentrations, which would not result in a change in energy transfer after cholesterol depletion. While the amount of integrin microclustering in the cell membrane is similar for all three cell lines before cholesterol depletion, the distribution of these microclusters into cholesterol dependent regions is not the same, as determined by different changes in energy transfer after cholesterol depletion. This fact may be due to the differences in the integrins' ligand affinity, which has been shown to alter the integrins' equilibrium conformation, and, as we suggest, their localization in the membrane. The integrin ligand affinity from lowest to highest is: wild-type, αanaβ, αβV409D. The amount of cholesterol dependent clustering from most clustered to least clustered: wild-type (-50%), αanaβ (0%, not statistically significant), αβV409D (+240%). Studies with additional integrin mutants could further test this hypothesis.

Previous studies have shown that treatment with mβCD can extract membrane phospholipids along with cholesterol (29), and that restoration of membrane properties, such

as diffusion coefficients, are achieved by restoring the cholesterol levels to their original values (22). The measured changes in membrane properties were confirmed to be the result of cholesterol extraction, and not another membrane component, by adding cholesterol back to the membrane to observe if the membrane properties were restored to the original values. The cholesterol depleted αβV409D expressing cells were incubated with chol-mβCD and cholesterol concentrations were measured as previously described. Figure 3 (dashed data bar) shows that the cholesterol level in cells expressing the αβV409D mutant integrins and FRET reporters can be restored to the level similar to untreated cells. The FRAP results (Table 1) indicate that the lipid diffusion coefficient for the αβV409D cell line is restored to a statistically same value compared to the untreated cells. Similarly, the FRET results (Table 2) indicate that αβV409D integrin microclustering levels return to the original value obtained for the untreated cells. These results confirm that the membrane properties being measured for this cell line are a result of altered cholesterol concentration in the membrane, and not from another membrane component(s) that may be simultaneously altered, since only cholesterol levels were restored to their original value.

CONCLUSIONS

Integrins are ubiquitous membrane receptors that are important in nearly all cell signaling cascades, including those that control basic cellular functions (55-57). Therefore, it is important to understand the molecular mechanism of integrin function. This not only includes the much studied changes in ligand affinity and macro-scale clustering, but also the lesser studied changes in receptor microclustering. The data reported herein highlights a

simple method that can be used to elucidate the role of cholesterol in wild-type integrin microclustering, and for integrins with altered signaling properties. Upon cholesterol depletion, the maximum change in integrin microclustering was measured for cells expressing αβV409D integrins, which have the highest affinity for ligand out of the three integrins included in this study. Restoring cholesterol to native levels also restored the levels of αβV409D integrin microclustering, indicating the measured changes are cholesterol-dependent. Similar FRET assays can be utilized to measure the role of cholesterol in the microclustering of integrins in other cell types and for other members of the integrin family. These assays are currently being developed.

ACKNOWLEDGMENTS

The support for this work was provided by the Roy J. Carver Charitable Trust (Muscatine IA), and the National Science Foundation (CHE-0845236). The authors thank Roger Tsien (Howard Hughes Medical Institute, La Jolla, CA) for the original mCherry plasmid, Atsushi Miyawaki (Riken, Wako-city, Saitama, Japan) for the original Venus plasmid, Christopher Gonwa-Reeves (Iowa State University) for assisting with the statistical analysis, and Anthony Young and Andrew Pavel for their assistance in lipid extraction and HPLC analysis.

REFERENCES

1. Giancotti, F. G., and E. Ruoslahti. 1999. Integrin signaling. Science 285:1028-1032.

2. Tang, C. K., and G. A. Pietersz. 2009. Intracellular detection and immune signaling pathways of DNA vaccines. Expert review of vaccines 8:1161-1170.

3. Su, C. Y., K. Menuz, and J. R. Carlson. 2009. Olfactory perception: receptors, cells, and circuits. Cell 139:45-59.

4. Sorkin, A., and M. von Zastrow. 2009. Endocytosis and signalling: intertwining molecular networks. Nature reviews 10:609-622.

5. Khan, W. N. 2009. B cell receptor and BAFF receptor signaling regulation of B cell homeostasis. J Immunol 183:3561-3567.

6. Van Kooyk, Y., and C. G. Figdor. 2000. Avidity regulation of integrins: the driving force in leukocyte adhesion. Current opinion in cell biology 12:542-547.

7. Saito, T., and T. Yokosuka. 2006. Immunological synapse and microclusters: the site for recognition and activation of T cells. Current opinion in immunology 18:305-313.

8. Vicente-Manzanares, M., and F. Sanchez-Madrid. 2004. Role of the cytoskeleton during leukocyte responses. Nat Rev Immunol 4:110-122.

9. Ginsberg, M. H., A. Partridge, and S. J. Shattil. 2005. Integrin regulation. Curr Opin Cell Biol 17:509-516.

10. Adair, B. D., and M. Yeager. 2007. Electron Microscopy of Integrins. Methods Enzymol 426:337-373.

11. van Kooyk, Y., S. J. van Vliet, and C. G. Figdor. 1999. The actin cytoskeleton regulates LFA-1 ligand binding through avidity rather than affinity changes. J Biol Chem 274:26869-26877.

12. Yauch, R. L., D. P. Felsenfeld, S. K. Kraeft, L. B. Chen, M. P. Sheetz, and M. E. Hemler. 1997. Mutational evidence for control of cell adhesion through integrin diffusion/clustering, independent of ligand binding. The Journal of experimental medicine 186:1347-1355.

13. Hato, T., N. Pampori, and S. J. Shattil. 1998. Complementary roles for receptor clustering and conformational change in the adhesive and signaling functions of integrin alphaIIb beta3. J Cell Biol 141:1685-1695.

14. Selvin, P. R. 2000. The renaissance of fluorescence resonance energy transfer. Nat Struct Biol 7:730-734.

15. Buensuceso, C., M. de Virgilio, and S. J. Shattil. 2003. Detection of integrin alpha IIbbeta 3 clustering in living cells. J Biol Chem 278:15217-15224.

16. Kim, M., C. V. Carman, W. Yang, A. Salas, and T. A. Springer. 2004. The primacy of affinity over clustering in regulation of adhesiveness of the integrin {alpha}L{beta}2. J Cell Biol 167:1241-1253.

17. Smith, E. A., T. A. Bunch, and D. L. Brower. 2007. General in vivo assay for the study of integrin cell membrane receptor microclustering. Anal Chem 79:3142-3147.

18. Dibya, D., S. Sander, and E. A. Smith. 2009. Identifying cytoplasmic proteins that affect receptor clustering using fluorescence resonance energy transfer and RNA interference. Analytical and bioanalytical chemistry 395:2303-2311.

19. Klappauf, E., and D. Schubert. 1977. Band 3-protein from human erythrocyte membranes strongly interacts with cholesterol. FEBS letters 80:423-425.

20. Muhlebach, T., and R. J. Cherry. 1982. Influence of cholesterol on the rotation and self-association of band 3 in the human erythrocyte membrane. Biochemistry 21:4225-4228.

21. McConnell, H. M., and M. Vrljic. 2003. Liquid-liquid immiscibility in membranes. Annual review of biophysics and biomolecular structure 32:469-492.

22. Vrljic, M., S. Y. Nishimura, W. E. Moerner, and H. M. McConnell. 2005. Cholesterol depletion suppresses the translational diffusion of class II major histocompatibility complex proteins in the plasma membrane. Biophysical journal 88:334-347.

23. Yeagle, P. L. 1985. Cholesterol and the cell membrane. Biochimica et biophysica acta 822:267-287.

24. Baird, B., E. D. Sheets, and D. Holowka. 1999. How does the plasma membrane participate in cellular signaling by receptors for immunoglobulin E? Biophysical chemistry 82:109-119.

25. Janes, P. W., S. C. Ley, A. I. Magee, and P. S. Kabouridis. 2000. The role of lipid rafts in T cell antigen receptor (TCR) signalling. Seminars in immunology 12:23-34.

26. Krauss, K., and P. Altevogt. 1999. Integrin leukocyte function-associated antigen-1-mediated cell binding can be activated by clustering of membrane rafts. J Biol Chem 274:36921-36927.

27. Simons, K., and D. Toomre. 2000. Lipid rafts and signal transduction. Nature reviews 1:31-39.

28. Tansey, M. G., R. H. Baloh, J. Milbrandt, and E. M. Johnson, Jr. 2000. GFRalpha-mediated localization of RET to lipid rafts is required for effective downstream signaling, differentiation, and neuronal survival. Neuron 25:611-623.

29. Kilsdonk, E. P., P. G. Yancey, G. W. Stoudt, F. W. Bangerter, W. J. Johnson, M. C. Phillips, and G. H. Rothblat. 1995. Cellular cholesterol efflux mediated by cyclodextrins. J Biol Chem 270:17250-17256.

30. Bunch, T. A., and D. L. Brower. 1992. Drosophila PS2 integrin mediates RGD-dependent cell-matrix interactions. Development 116:239-247.

31. Jannuzi, A. L., T. A. Bunch, M. C. Brabant, S. W. Miller, L. Mukai, M. Zavortink, and D. L. Brower. 2002. Disruption of C-terminal cytoplasmic domain of betaPS integrin subunit has dominant negative properties in developing Drosophila. Molecular biology of the cell 13:1352-1365.

32. Jannuzi, A. L., T. A. Bunch, R. F. West, and D. L. Brower. 2004. Identification of integrin beta subunit mutations that alter heterodimer function in situ. Molecular biology of the cell 15:3829-3840.

33. Bligh, E. G., and W. J. Dyer. 1959. A rapid method of total lipid extraction and purification. Canadian journal of biochemistry and physiology 37:911-917.

34. Amundson, D. M., and M. Zhou. 1999. Fluorometric method for the enzymatic determination of cholesterol. Journal of biochemical and biophysical methods 38:43-52.

35. Reits, E. A., and J. J. Neefjes. 2001. From fixed to FRAP: measuring protein mobility and activity in living cells. Nature cell biology 3:E145-147.

36. Zal, T., and N. R. Gascoigne. 2004. Photobleaching-corrected FRET efficiency imaging of live cells. Biophysical journal 86:3923-3939.

37. Gordon, G. W., G. Berry, X. H. Liang, B. Levine, and B. Herman. 1998. Quantitative fluorescence resonance energy transfer measurements using fluorescence microscopy. Biophysical journal 74:2702-2713.

38. Bland, J. M., and D. G. Altman. 1996. The use of transformation when comparing two means. BMJ (Clinical research ed 312:1153.

39. Altman, D. G., S. M. Gore, M. J. Gardner, and S. J. Pocock. 1983. Statistical guidelines for contributors to medical journals. British medical journal (Clinical research ed 286:1489-1493.

40. Zar, J. 1999. Biostatistical Analysis Prentice Hall, Upper Saddle River, NJ.

41. Martin-Bermudo, M. D., and N. H. Brown. 1996. Intracellular signals direct integrin localization to sites of function in embryonic muscles. J Cell Biol 134:217-226.

42. Brower, D. L. 2003. Platelets with wings: the maturation of Drosophila integrin biology. Curr Opin Cell Biol 15:607-613.

43. Clark, A. J., and K. Block. 1959. The absence of sterol synthesis in insects. J Biol Chem 234:2578-2582.

44. Dobrosotskaya, I. Y., A. C. Seegmiller, M. S. Brown, J. L. Goldstein, and R. B. Rawson. 2002. Regulation of SREBP processing and membrane lipid production by phospholipids in Drosophila. Science 296:879-883.

45. Bunch, T. A., T. L. Helsten, T. L. Kendall, N. Shirahatti, D. Mahadevan, S. J. Shattil, and D. L. Brower. 2006. Amino acid changes in Drosophila alphaPS2betaPS integrins that affect ligand affinity. J Biol Chem 281:5050-5057.

46. Connor, J., C. Bucana, I. J. Fidler, and A. J. Schroit. 1989. Differentiation-dependent expression of phosphatidylserine in mammalian plasma membranes: quantitative assessment of outer-leaflet lipid by prothrombinase complex formation. Proceedings of the National Academy of Sciences of the United States of America 86:3184-3188.

47. Hotta, K., B. Bazartseren, Y. Kaku, A. Noguchi, A. Okutani, S. Inoue, and A. Yamada. 2009. Effect of cellular cholesterol depletion on rabies virus infection. Virus research 139:85-90.

48. Baier, C. J., C. E. Gallegos, V. Levi, and F. J. Barrantes. 2009. Cholesterol modulation of nicotinic acetylcholine receptor surface mobility. Eur Biophys J.

49. Hansen, G. H., L. L. Niels-Christiansen, E. Thorsen, L. Immerdal, and E. M. Danielsen. 2000. Cholesterol depletion of enterocytes. Effect on the Golgi complex and apical membrane trafficking. J Biol Chem 275:5136-5142.

50. Pucadyil, T. J., and A. Chattopadhyay. 2006. Effect of cholesterol on lateral diffusion of fluorescent lipid probes in native hippocampal membranes. Chemistry and physics of lipids 143:11-21.

51. Zhai, L., D. Chaturvedi, and S. Cumberledge. 2004. Drosophila wnt-1 undergoes a hydrophobic modification and is targeted to lipid rafts, a process that requires porcupine. J Biol Chem 279:33220-33227.

52. Klein, C., T. Pillot, J. Chambaz, and B. Drouet. 2003. Determination of plasma membrane fluidity with a fluorescent analogue of sphingomyelin by FRAP measurement using a standard confocal microscope. Brain research 11:46-51.

53. Ramprasad, O. G., N. Rangaraj, G. Srinivas, J. P. Thiery, S. Dufour, and G. Pande. 2008. Differential regulation of the lateral mobility of plasma membrane phospholipids by the extracellular matrix and cholesterol. Journal of cellular physiology 215:550-561.

54. Wolf, D. E., S. S. Hagopian, and S. Ishijima. 1986. Changes in sperm plasma membrane lipid diffusibility after hyperactivation during in vitro capacitation in the mouse. J Cell Biol 102:1372-1377.

55. Harburger, D. S., and D. A. Calderwood. 2009. Integrin signalling at a glance. Journal of cell science 122:159-163.

56. Huveneers, S., and E. H. Danen. 2009. Adhesion signaling - crosstalk between integrins, Src and Rho. Journal of cell science 122:1059-1069.

57. Legate, K. R., S. A. Wickstrom, and R. Fassler. 2009. Genetic and cell biological analysis of integrin outside-in signaling. Genes & development 23:397-418.

Table 1. Lipid diffusion coefficients measured by FRAP for the untreated cells, cholesterol depleted cells and (αβV409D cell line only) cholesterol restored cells

Cell Lines	Untreated cells (cm^2/s)	Cholesterol depleted cells (cm^2/s)	p-value *	Cholesterol restored cells (cm^2/s)	p-value *
αβ Reporters	1.91×10^{-9}	2.41×10^{-9}	0.048	-	-
αanaβ Reporters	1.95×10^{-9}	2.36×10^{-9}	0.0095	-	-
αβV409D Reporters	2.03×10^{-9}	2.81×10^{-9}	0.0004	1.94×10^{-9}	0.37

* The data for cholesterol depleted/restored cells has been statistically compared with the untreated data set and the statistical significance is represented by the p-values

Table 2. Integrin microclustering levels measured by FRET for the untreated cells, cholesterol depleted cells and (αβV409D cell line only) cholesterol restored cells

Cell Lines	Untreated cells	Cholesterol depleted cells	p-value *	Cholesterol restored cells	p-value *
αβ Reporters	0.010	0.005	0.020	-	-
αanaβ Reporters	0.011	0.014	0.36	-	-
αβV409D Reporters	0.008	0.026	0.0001	0.006	0.45

* The data for cholesterol depleted/restored cells has been statistically compared with the untreated data set and the statistical significance is represented by the p-values

Figure 1. Schematic of the FRET assay used to measure integrin microclustering with donor and acceptor FRET reporters. Energy transfer is measured (Top) prior to altering the plasma membrane cholesterol level; (Middle) after reducing the concentration of cholesterol by approximately 50%; and (Bottom) after restoring cholesterol levels to approximately the starting concentration before treatment.

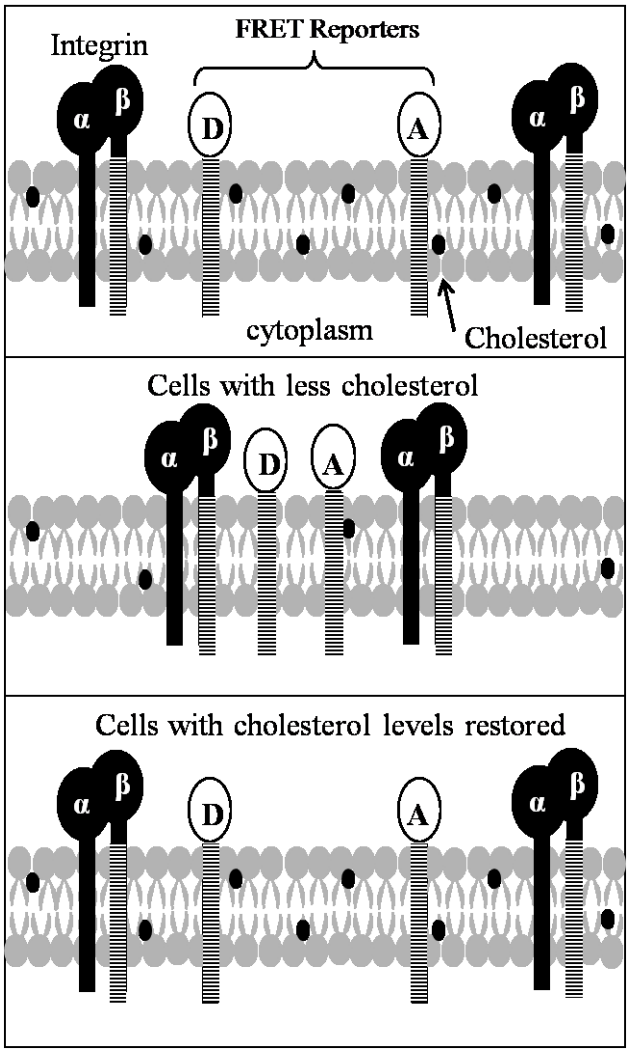

Figure 2. Schematic showing the steps to alter the cholesterol levels in *Drosophila* S2 cells. Cyclodextrins (methyl-β cyclodextrin) were used to reduce the concentration of cholesterol in live cells, followed by addition of cholesterol (Chol-mβCD) to the growth medium to restore cholesterol levels. In each cell population, integrin microclustering and lipid diffusion were measured with FRET and FRAP, respectively.

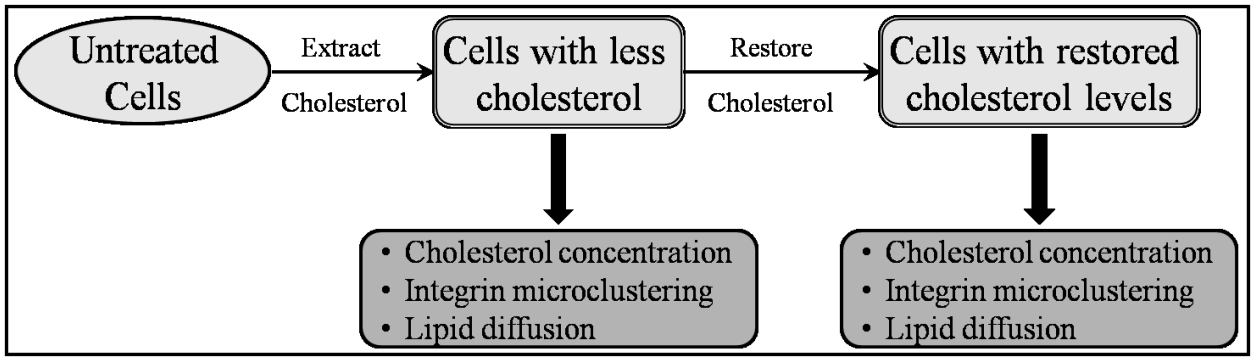

Figure 3. Graph of the amount of cholesterol measured per cell in three cell populations (black) untreated cells before cholesterol reduction; (white) after reduction with mβCD to extract cholesterol; and (dashed) after adding chol-mβCD to the growth medium to restore cholesterol levels. Error bars represents three replicate experiments. Details of the cell lines are found in the text.

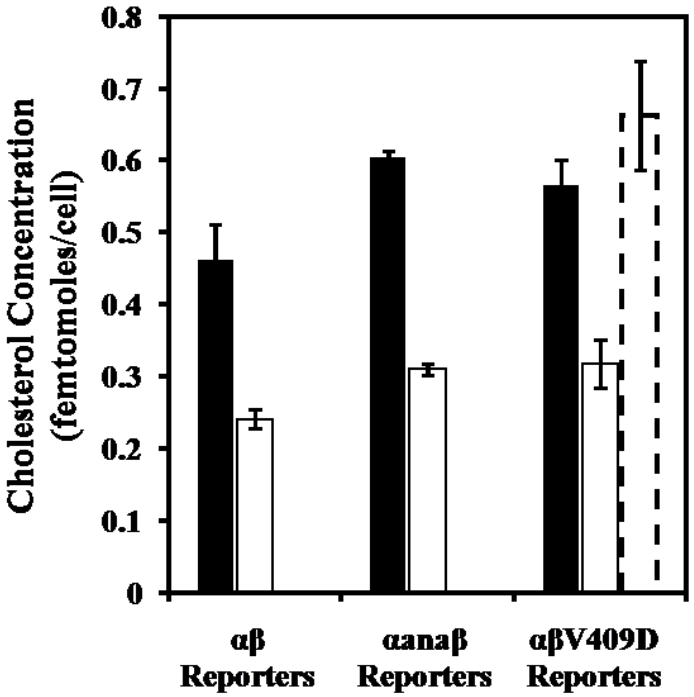

Figure 4. Graph of the amount of cholesterol measured per αβV409D integrin expressing cell after adding additional cholesterol to the growth medium. The basal concentration of cholesterol in the growth medium is 45 μM. Error bars represents three replicate experiments.

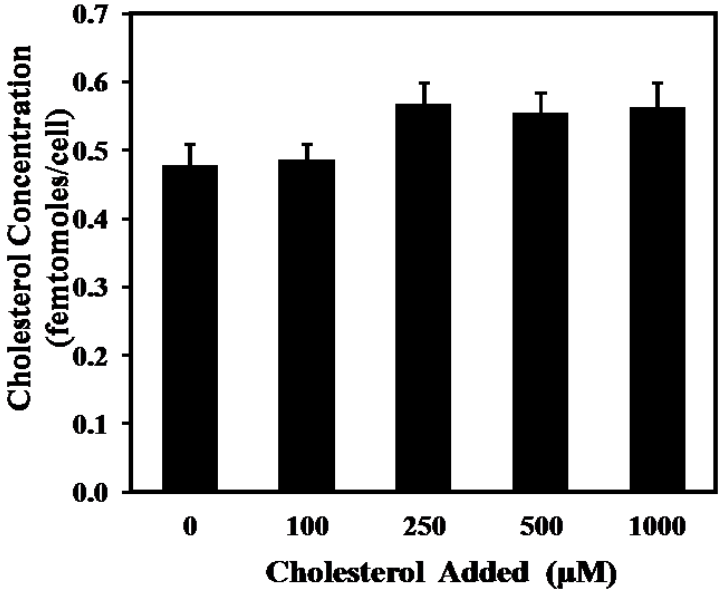

Supplementary Figure S1. Chromatogram of lipid extract from transformed *Drosophila* S2 cells. Traces represent lipid extract from cells and lipid extract spiked with a cholesterol standard. Lipid extracts obtained with the Bligh-Dyer method, were analyzed using High Performance Liquid Chromatography (HPLC) with a UV-Vis detector (Agilent, USA). A reverse phase C-18 column (ZORBAX Eclipse XDB-C18, 4.6x150mm, 5 µm) was used with a flow rate of 1.0 ml/min. The absorbance was monitored at 205 nm wavelength. The mobile phase solvents consisted of 3 % water and the remaining 97% consisted of acetonitrile/methanol (50/50, v/v). 5 µL of the lipid extract was injected into the column.

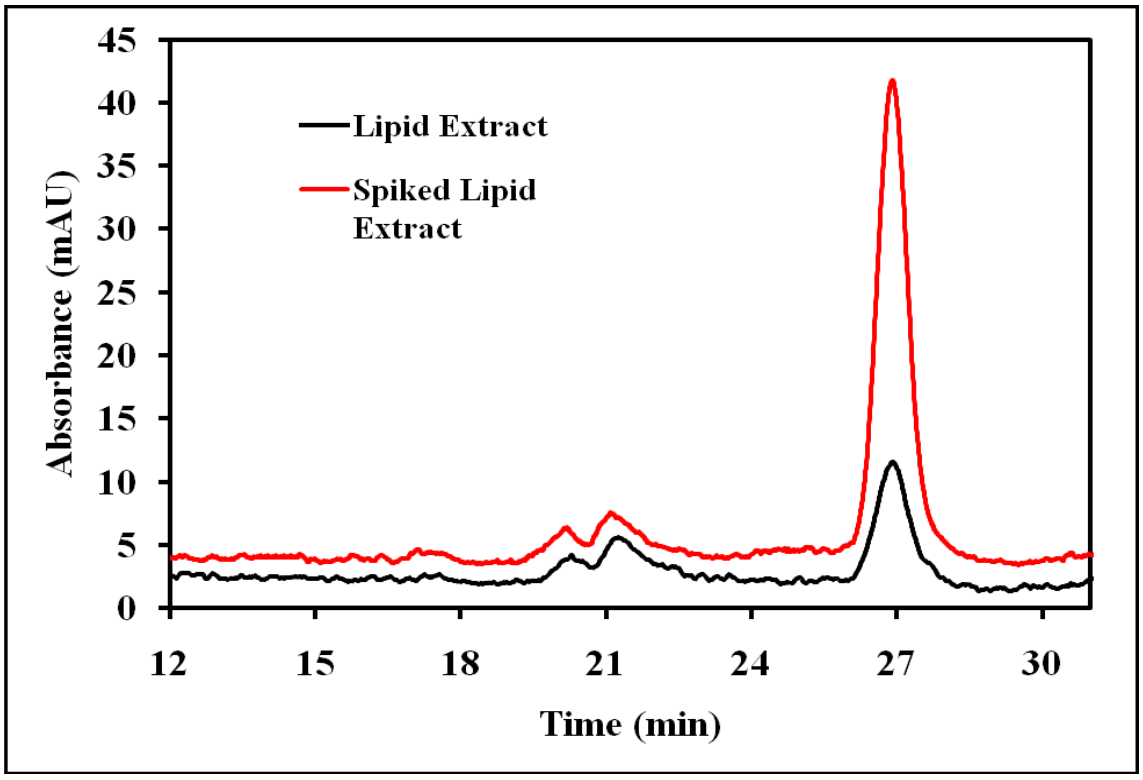

Supplementary Figure S2. Calibration curve obtained using an Amplex red assay and cholesterol standards. Error bars represent three replicate experiments.

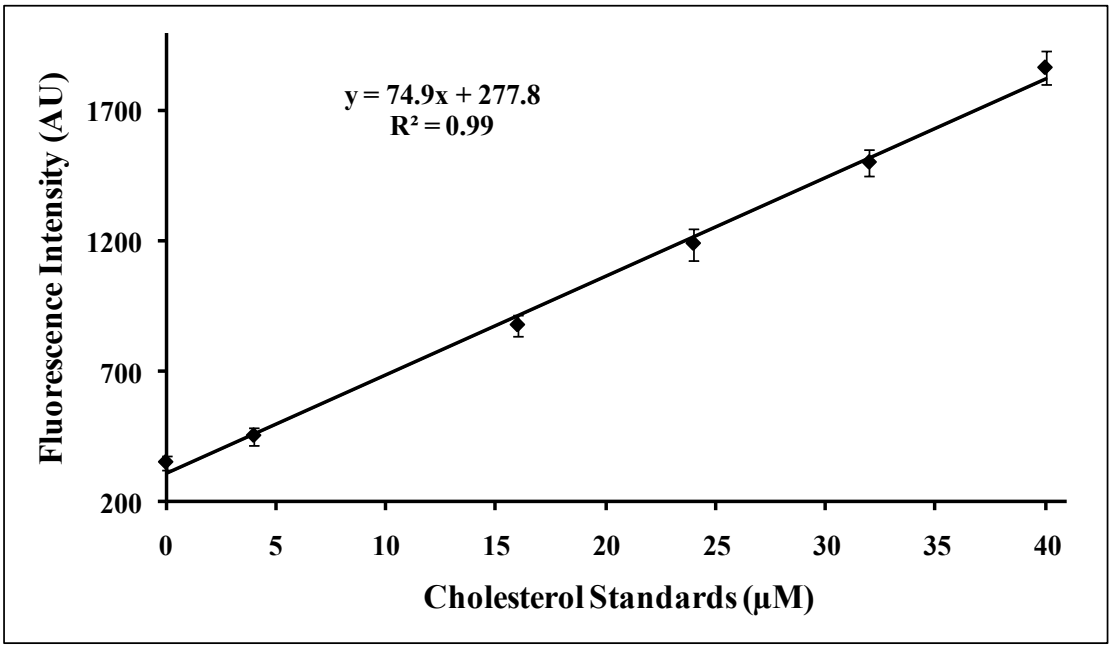

Supplementary Figure S3. Example of FRAP curve showing the changes in fluorescence intensity for the photobleached spot (triangles) on membrane of cells expressing wild-type integrins. Carbocyanine DiD is used to dye the membrane. Initial four data points represent pre-photobleached spot. Approximately 70% decrease in fluorescence intensity is observed immediately after photobleaching. Over time the photobleached spot is repopulated with unbleached DiD dye molecules and full recovery is begins within ~6 seconds of photobleaching. The difference between recovered and the pre-bleached intensity shows a ~20% immobile fraction within the membrane. The experimental data was fitted to an exponential curve. The dotted lines is plotted to obtain the time at which the 50% of the recovery was achieved, which is used to calculate the diffusion coefficient.

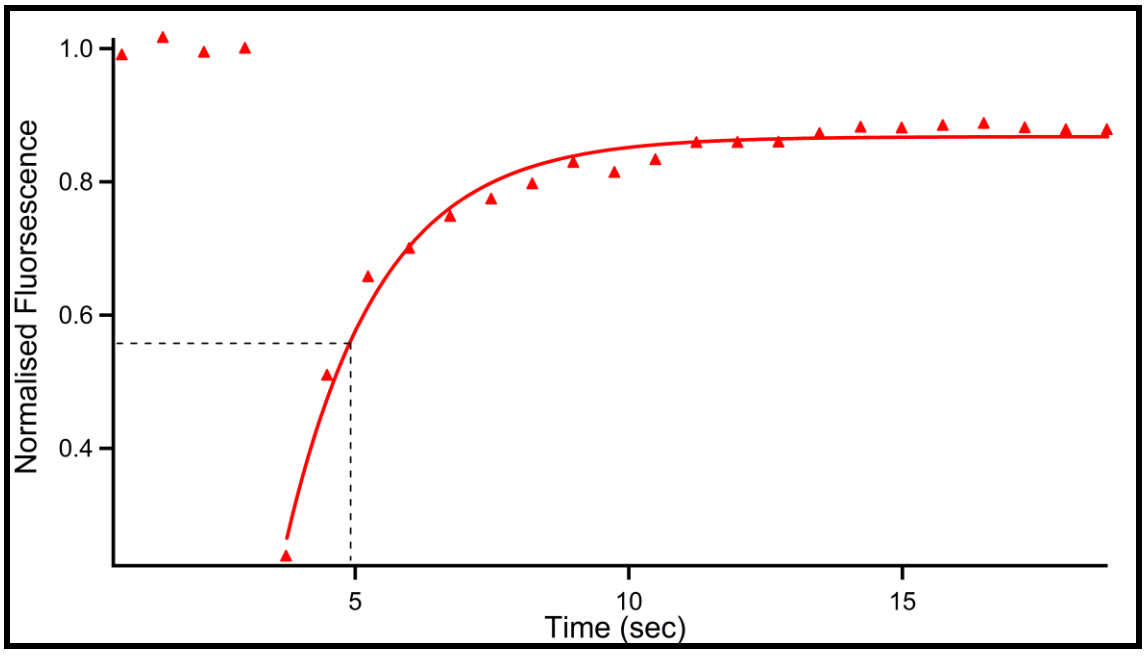

CHAPTER 4: GENERAL CONCLUSIONS AND FUTURE PROSPECTS

GENERAL CONCLUSIONS

Currently, few analytical techniques can measure nanoscale events in an in-vivo environment leading to a better understanding of the organization of the cell membrane. The work presented in this thesis describes how intracellular signaling events can be measured by coupling the FRET and RNAi techniques. The ability to measure intracellular signaling events opens the way to further investigate other signaling pathways using this approach. Also, the dissertation describes how cholesterol sequestration is combined with FRET to deduce the role of cholesterol in the cell signaling.

The second chapter focuses on combining FRET with RNAi to measure integrin microclustering without altering the integrin dynamics. The data presented herein revealed that four cytoplasmic proteins involved in connecting integrins with the actin cytoskeleton also affect integrin microclustering when extracellular signaling events are minimal. The results also indicated that αβV409D mutant integrin is more sensitive to interactions linking integrins to receptor tyrosine kinases (RTK) compared to wild-type integrins. For alpha cytoplasmic mutation (αanaβ integrins), the data indicated no change in microclustering when expression of all the cytoplasmic proteins except paxillin is reduced.

The data reported in chapter three elucidates the role of cholesterol in integrin microclustering. This study reports the alterations in integrin microclustering in response to cholesterol depletion and restoration**.** Quantitative changes in integrin microclustering and lipid diffusion are measured when more than 40% membrane cholesterol is depleted. More than 20% increase in lipid diffusion, at reduced cholesterol levels, was observed for the cells

expressing wild-type or mutant integrins. Upon cholesterol depletion, maximum change in lipid diffusion and energy transfer is observed for cells expressing αβV409D integrins, which have the highest ligand affinity of the three integrins studied here. The reversibility of the process was assessed by reintroducing cholesterol in the cholesterol depleted cells. Both the lipid diffusion and the integrin microclustering are restored in the cells expressing the αβV409D integrins, indicating the measured changes are cholesterol dependent. Because of the limited uptake of cholesterol by S2 cells, measuring integrin microclustering under more than normal cholesterol levels were not possible.

FUTURE PROSPECTS

The scope of the developed method described in this dissertation is not just limited to measuring integrin microclustering under altered levels of cholesterol and cytoplasmic proteins. The method demonstrated herein can be applied in many different combinations to determine various factors that affect integrin microclustering.

Previous studies by Smith et al. showed the dependence of αβV409D mutant integrin microclustering on the presence of other membrane proteins.[1] In Chapter 2 (Figure 4) the FRET results for αβV409D mutant revealed that the receptor tyrosine kinase (RTK) can possible affect integrin function. This FRET data can be used as a preliminary evidence to target the RTK, using RNAi, and measure the subsequent changes in integrin microclustering. Another membrane protein that can be studied is insulin like receptor (InR), which has been previously shown to be associated with integrins and are natively expressed in S2 cells.[2] A class of membrane proteins called tetraspanins is known to interact with the alpha subunit of integrins and also forms web like complexes among themselves and with

integrins.[3] Studying the integrin function under reduced expression of one or more tetraspanins can provide useful insights into the interplay between integrins and tetraspanins.

The method can be further extended to observe the changes in integrin microclustering under the simultaneous reduced expression of both the membrane proteins and cytoplasmic proteins. Based on this thesis finding and a known previous relationship between DOCK and RTK, valuable information can be obtained by targeting DOCK and RTK simultaneously and measuring the αβV409D mutant integrin microclustering.

As an extension to the approach presented in this dissertation, coupling the three techniques FRET assay, RNAi technique and cholesterol sequestration can unravel complex interactions between the integrins and other cellular components. Additionally, a more complex connection can be made between intracellular signaling events and extracellular signaling events by performing the experiments in chapter 2 at high ligand density.

Integrins are not the only class of receptors that can be studied using the FRET reporters. Other receptors can also be studied using appropriately designed FRET reporters. A good choice will be an important class of receptors called EGFR.

REFERENCES

(1) Smith, E. A.; Bunch, T. A.; Brower, D. L. (2007) General in vivo assay for the study of integrin cell membrane receptor microclustering, *Anal Chem*, 79, 3142-3147.

(2) Krishnamoorthy, S. (2008) Receptor tyrosine kinase (RTK) mediated tyrosine phosphor-proteome from Drosophila S2 (ErbB1) cells reveals novel signaling networks, *PLoS One*, 3, e2877.

(3) Levy, S.; Shoham, T. (2005) Protein-protein interactions in the tetraspanin web, *Physiology (Bethesda)*, 20, 218-224.

APPENDIX I: Statistical Analysis of FRET and FRAP data

Deepak Dibya and Emily A. Smith

In order to statistically analyze the skewed data, the data can be reduced by transforming the data thereby reducing the skewness. The mathematical transformations that can be applied to the data include square root, reciprocal, logarithm etc. If a transformation is used, it is important to check whether the normal distribution of the data is achieved after the transformation or not.

All the FRET and the FRAP data presented in this dissertation has been statistically analyzed using the application JMP 7 (SAS Institute Inc, Cary, USA), with statistical consulting through the Iowa State University Department of Statistics. An example of the statistical analysis of the FRET data is presented in this appendix.

Open the JMP 7.0 program and follow the steps to statistically analyze the data.

1. File>New>Data table

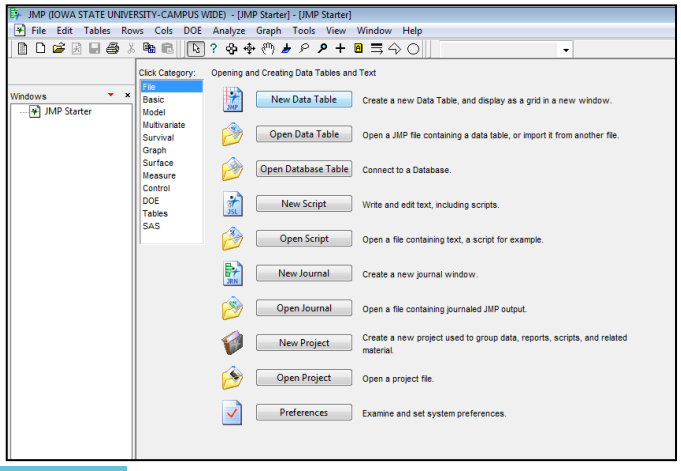

2. Select `Cols>Add New Column`. The next window prompts to name the new column and provide column characteristics. Ensure that the `data type` is set to `numeric` and `Modeling` is `continuous`.

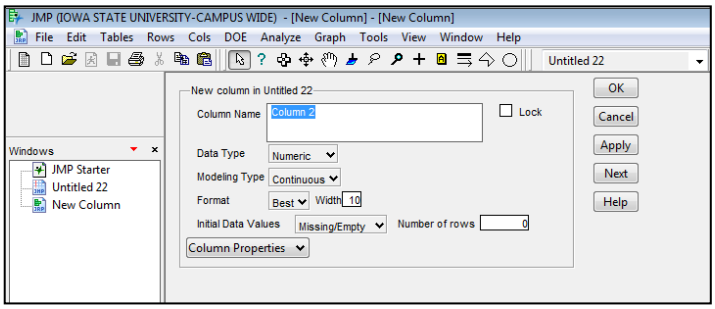

3. Double click on `Column 1`. Change the `data type` to `character` and `modeling type` to `Nominal`.

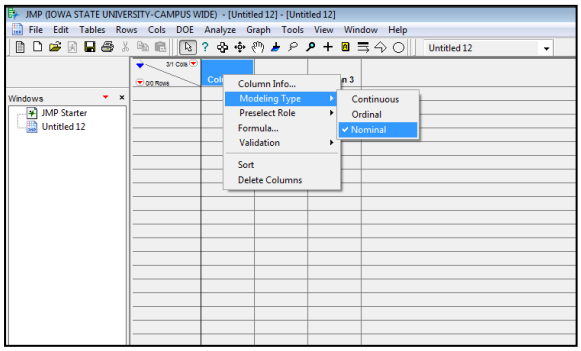

4. After assigning the modeling types to the columns, begin data analysis by pasting the data in `Column 2`; one data set followed by the other. `Column 1` contains the information given by data in `Column 2`, where control and experiment are represented by 0 and 1 in `Column 1` respectively. The cells in the columns with dots showing no data are not included when analyzing the data.

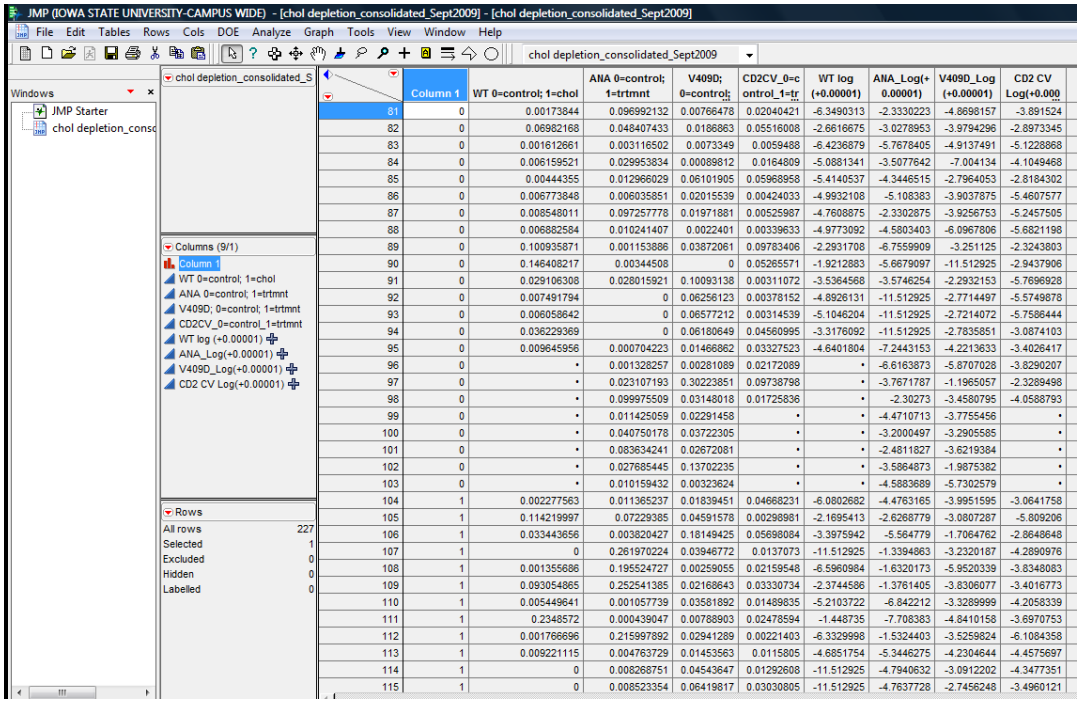

5. The normal distribution of the data can be determined by using the menu function `Analyze>Distribution` and selecting `Column 1` as `By` and data columns as `Y, Columns.`

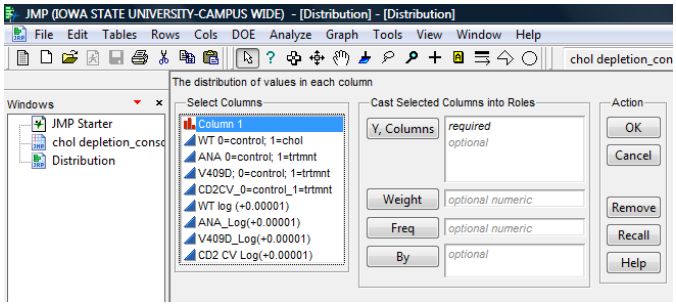

6. The distribution function shows that the raw data is not normally distributed (Figure 1, Column 2) which means statistical tests like t-test cannot be utilized for data analysis. The normal distribution was achieved by taking the natural log of the raw

data (Figure 1, Column 3), and the means were compared using Welch's *t*-test on the transformed data.

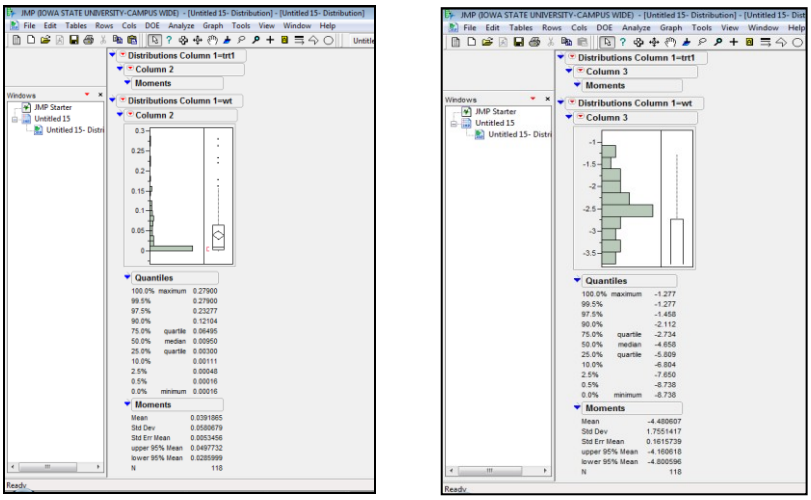

Figure 1. Distribution of raw data (column 2) and log transformed data (column 3)

7. In order to perform t-test, select `Analyze>Fit X by Y` and use `Column 1` as `X factor` and data sets as `Y, Response.` Click on the small red triangle at the corner of the plot, then select `UnEqual Variances`

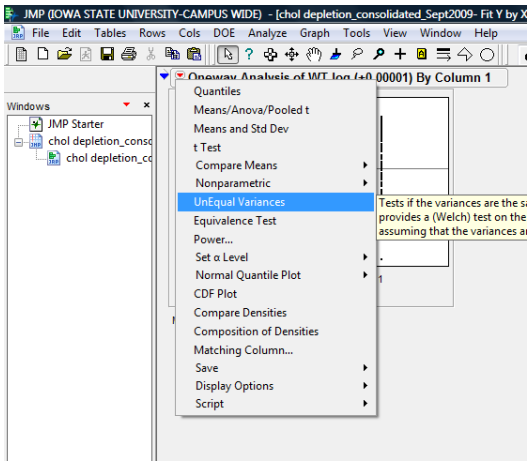

8. This (as shown in figure below) presents the results of statistical analysis that can now be used to interpret the data.

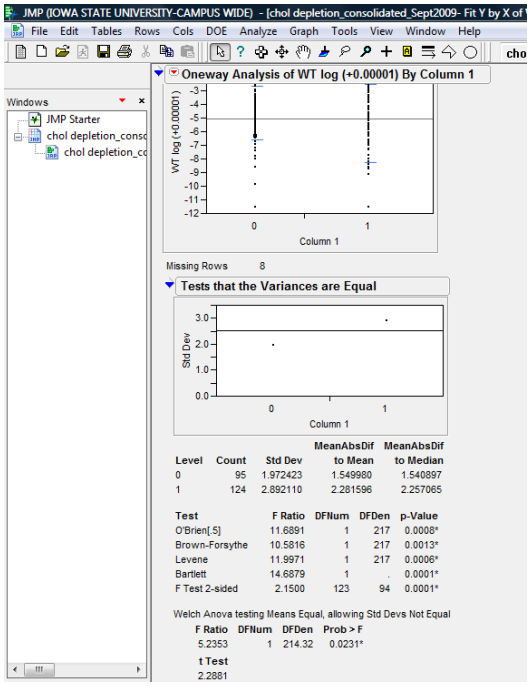

The Welch *t*-test is a modification of the student *t*-test and does not assume equal variances. Results of the Welch *t*-test are reported as p-values. A p-value of less than 0.05 suggests that the two means are different. Moreover, a p-value of more than 0.05 does not indicate that the two means are same. It means that there is not enough statistical evidence to show that the two means are different. Two means with a p-value of greater than 0.05 can be statistically different if the sample size under analysis was too small or the null hypothesis is really true. This would require advance statistical analysis of the data.

APPENDIX II: Expression, Purification and Estimation of Taq DNA Polymerase

Deepak Dibya and Emily A. Smith

INTRODUCTION

Polymerase chain reaction (PCR) is a well known reaction invented by Kary Mullis in 1985 for the *in-vitro* amplification of DNA sequences. Figure below shows how this technique can be utilized in making large number of copies of a gene from a template DNA.

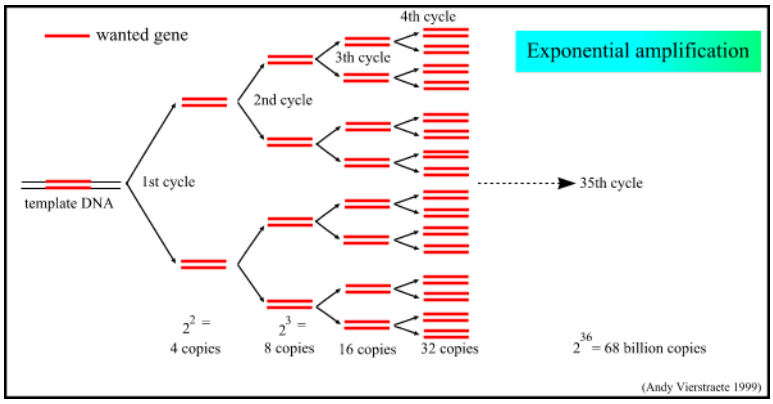

Adapted from the homepage of Andy Vierstraete

There are several chemicals and enzymes required to complete the PCR. One of the key components in duplicating DNA sequences in PCR is an enzyme called Taq polymerase. This enzyme has been isolated previously and is widely used in PCR based applications. Taq

polymerase is a thermostable enzyme and can survive the temperature fluctuations involved in PCR. The enzyme participates in a template directed syntheses of DNA fragments and requires free Mg^{2+} for its optimum functioning.

The protocol for making Taq polymerase is well developed and is routinely used in academia and industry to express and purify the enzyme. Since commercial Taq polymerase is expensive, Taq polymerase was prepared in Smith group at Iowa State University

EXPERIMENTAL

Taq polymerase synthesis is a four step process. First, bacterial cell culture media is prepared to grow DH5α *E.coli* cells that contains plasmid specific for Taq polymerase. The second step involves the expression of Taq polymerase in the confluent cell culture by chemical induction. This is followed by purification of the enzyme. Finally the efficacy of the purified enzyme is validated by performing a PCR reaction and analyzing the PCR products in on a agarose gel electrophoresis. Also, the efficiency of the enzyme is compared with commercially available enzyme and an optimum amount of enzyme is estimated to conduct future PCR reactions.

Preparation of terrific broth (media)

Taq polymerase was purified from DH5α *E.coli* cells expressing the inserted plasmid specific for Taq polymerase. The cells were grown in terrific broth media. To make terrific

broth media,12 g bactotryptone, 24 g yeast extract and 4 mL glycerol were dissolved in 900 mL water and sterilized. To this sterilized solution, 100 mL sterile solution of 0.17 M KH_2PO_4 and 0.72 M K_2HPO_4 was added. Antibiotic used for pTaq was ampicillin. Ampicillin was not added to the entire solution but to only that portion of the media that was used for growing cells.

Expression of Taq polymerase

1.0 µL of 50 mg/mL ampicillin solution was added to 1.0 mL of the terrific broth media. The media was inoculated with DH5α *E. coli* cells and incubated overnight at 37°C. 100 µl of this culture was used to inoculate a fresh 1.0 mL culture media containing 1.0 µL of 50 mg/mL ampicillin. It was then followed by incubation for 90 min at 37°C. This culture was transferred to a 100 mL fresh culture media (pre-warmed to 37°C in an incubator) containing 100 µL of 50 mg/mL ampicillin. The above culture was incubated at 37°C until an OD600 of 0.3 and then induced with 25 µL of 2.0 M IPTG. The culture was again incubated for 16 hours at 37°C and then centrifuged at 5000 rpm for 5 minutes to obtain a pellet of cells.

Purification of Taq polymerase

The pellet obtained from the culture was resuspended in 3 mL of Buffer A (50 mM Tris pH 7.9, 50 mM dextrose,1.0 mM EDTA, 4mg/mL lysosyme) and incubated for 15 min

at room temperature. To this was added 3.0 mL of buffer B (10.0 mM Tris pH 7.0, 50 mM KCl, 1.0 mM EDTA, 0.5% Tween20, 0.5% Noni P40) and the solution was incubated for 60 min at 75°C with shaking. It was followed by centrifugation at 10000 rpm for 10 minutes to remove cell debris and denatured protein. The lysate was mixed with an equal volume of storage buffer (50 mM Tris pH 8.0, 100 mM NaCl, 0.1 mM EDTA, 0.5 mM Dithiothreitol (DTT) and 1% triton X-100) containing 50% glycerol. Equal volume of storage buffer containing 75% glycerol was again added. The resulting solution contained Taq polymerase, which was aliquoted and stored at -20°C.

RESULTS

Efficiency of the purified Taq polymerase (in-house) was verified by performing a PCR reaction and analyzing the PCR products on a 1% agarose gel electrophoresis. Serial dilution of the enzyme was used to establish an optimum volume of in-house Taq polymerase to be used for future PCR reactions. The in-house Taq was also compared with the

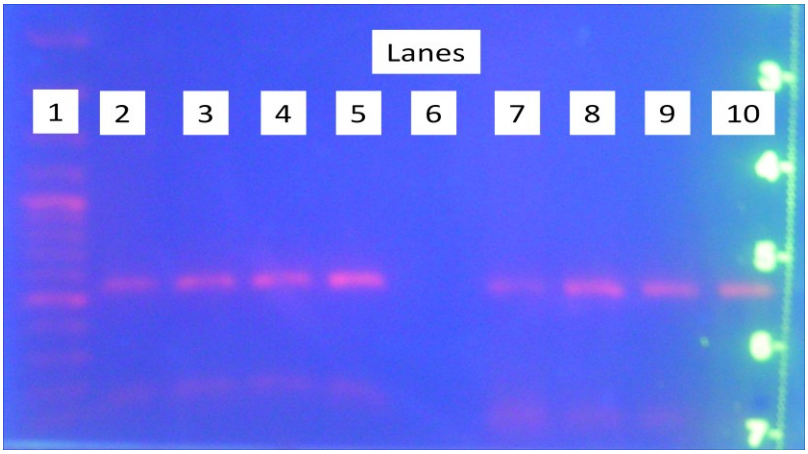

Figure 1. Gel electrophoresis of PCR products
Lane 1: Marker (ladder) lane
Lane 2-5: Higher to lower amounts of commercial Taq
Lane 6: Control (no Taq used in the PCR)
Lane 7-10: Higher to lower amounts of in-house Taq

commercially available Taq to estimate the amount of in-house Taq that will be needed for conducting PCR reactions successfully in future. Figure above is an agarose gel electrophoresis image showing the DNA fragments amplified by PCR using commercial Taq (Takara, WI) and in-house Taq.

APPENDIX III: Synthesis of double stranded RNA

Deepak Dibya and Emily A. Smith

INTRODUCTION

Double stranded RNA (dsRNA) was synthesized using the DNA sequences that correspond to the proteins targeted in Chapter 2. In brief, DNA sequences from S2 genomic DNA were amplified using polymerase chain reaction (PCR). The DNA amplicons were used as templates for single-stranded RNA (ssRNA) syntheses using MEGASCRIPT T7 Transcription Kit (Ambion, Austin, TX). ssRNA was purified by ethanol-precipitation, followed by the formation of dsRNA. The concentration of ssRNA was measured using UV-Vis spectrophotometry. The dsRNA products were also analyzed with 1% agarose gel electrophoresis.

The enzyme that catalyzes the formation of ssRNA in the 5'→ 3' direction is called T7 RNA polymerase. T7 RNA polymerase is extremely promoter-specific and only transcribes DNA cloned downstream of a T7 promoter region. The source of the enzyme is the T7 bacteriophage, a virus that infects only bacteria, and has been found to have a very low error rate. The molecular weight of this enzyme is 99kDa. In biotechnology applications, T7 RNA polymerase is commonly used to transcribe a DNA template into a ssRNA. The T7

promoter sequence used in all the primers herein is TAATACGACTCACTATAGGG. This T7 sequence was prefaced to every RNAi probe (forward and reverse primer sequence) that was used to target cytoplasmic proteins. Details of the RNAi probes used in synthesizing dsRNA are given in Table 1.

Table 1. RNAi probes. The letters F an R in the parentheses denote forward and reverse primers respectively.

Protein	Probe ID	Probe Length	Primer Sequence
Rhea (F)	HFA11300	507	CGCCGATCCAGGTCAAC
Rhea (R)			ATCATTTGCGGCTTAGTAGA
FAK (F)	BKN21731	529	TGATTGAACCTTGCACCAAA
FAK (R)			AACCAGGTCGACAAACGAAC
Paxillin (F)	BKN29242	313	TGTGGGATTGGGTCGTAAAT
Paxillin (R)			CCTTCTTTGATCACGAGGG
Vinculin (F)	HFA18728	513	CTTCAGCACCCGGAAATC
Vinculin (R)			GCGACCAGCGCTGATAA
Dreadlock (F)	HFA00812	440	TGTACAGCTTCACGTCAAACAA
Dreadlock (R)			AGTCTCACTGTCTCTGATGAG
Integrin linked kinase (F)	HFA11868	489	GGTAAACGAGCATGGAAACAC
Integrin linked kinase(R)			GAATTGCATGCTCCAATAATA
Steamer Duck (F)	HFA17070	269	CTTCCAGGATGGGATATTC
Steamer Duck (R)			CATAGCGGCCGGTAATCT

Further details of the RNAi probes such as efficiency and other target values are published elsewhere and can be obtained from the online resources: http://flyrnai.org

DNA amplicons

The genomic DNA extracted from S2 cells was used in a PCR along with the RNAi probes to amplify DNA sequences that correspond to the target cytoplasmic proteins. These DNA amplicons were later used as templates for the synthesis of ssRNA. The optimal concentration of genomic DNA used in PCR has been determined earlier. The DNA amplicons were stored at -20 °C for future use. The PCR conditions used for amplifying the DNA sequences are given in Table 2. These conditions have been optimized previously, by me, to yield optimum amplicons.

Table 2. PCR conditions for amplifying DNA sequences corresponding to Rhea

Stages	Steps	Temperature °C	Time (sec)	Number of Cycles
Stage 1	1	94	240	1
	2	0	0	
Stage 2	1	94	30	5
	2	51	05	
	3	72	30	
	4	0	0	
Stage 3	1	94	30	30
	2	65	05	
	3	72	30	
	4	0	0	
Stage 4	1	72	180	1
	2	0	0	

Concentration of DNA amplicons were estimated on a 1% agarose gel, using the intensity at 500bp of the ladder sequences. This concentration was used to estimate the amount of amplicon to be used in the subsequent step of ssRNA synthesis.

ssRNA synthesis

Enzyme mixture and the DNA amplicons were thawed on ice. 10X buffer provided in the kit was thawed at room temperature. The four nucleotides were thawed at room temperature and then put on ice. Table 3 shows the reaction mixture for synthesizing ssRNA for a cytoplasmic protein. The strategies described here were used in synthesizing ssRNA of all the seven cytoplasmic proteins targeted, as described in chapter 2. In Table 3, the contents in a 1.7 mL centrifuge tube were mixed by vortexing and combined in the order from top to bottom. Total volume of the reaction was kept at 20 µL.

Table 3. The reaction mixture for the synthesis of ssRNA. Master mix is the solution obtained by mixing equal amount of each of the nucleotides (U,A,G,C).

Reaction Components	**Cytoplasmic Proteins**	**Control**
Nucleotides (from master mix)	8 µL	8 µL
10 X buffer	2 µL	2 µL
DNA amplicon	8 µL	-
Enzyme (Ambion)	2 µL	2 µL
water	-	8 µL
Total Volume	20 µL	20 µL

The reaction mixture was incubated in a dry bath (should contain water) at 37 °C for 6 hours to overnight. After incubation, the solution volume was brought to 300µL by adding 240 µL of sterile water and 40 µL of 3.0 M sodium acetate (pH 5.2). Then 700µL of 200 proof ethanol was added. The contents were mixed and the tubes were kept in the freezer for at least 30 min and then centrifuged at the maximum speed (15,000 rpm) for 15 minutes at 4 °C. The supernatant was removed by decanting, followed by addition of 1 mL of 70% ice-cold ethanol. Again, the tubes were centrifuged at maximum speed for 15 min at 4 °C and the supernatant was removed. The resulting ssRNA pellet was resuspended in 50 µL of sterile water. At this time, the ssRNA is very susceptible to degradation; therefore the next steps should be done in quick succession.

For the UV-Vis measurement, 2.0 µL of the above ethanol precipitated ssRNA was diluted by adding 2.0 µL of the ssRNA to 348 µL of sterile water. Prior to the UV-Vis absorbance measurements, dsRNA was generated from the ssRNA by incubating the remaining ssRNA solution (48 µL) in the dry bath at 65°C for 30 min. After 30 min the metal holder containing the dsRNA centrifuge tube was taken out and allowed to cool at room temperature. During 30 min of dsRNA formation, absorbance measurements at 280 nm were taken and the concentration of the ssRNA was obtained. dsRNA solution was then diluted with sterile water to a final concentration of 1.0 µg/µL. This solution was analyzed on a 1% agarose gel to ensure that the dsRNA contained the desired number of base pairs. The dsRNA solution was stored at -20°C for future use.

VITA

NAME OF AUTHOR: Deepak Dibya

EDUCATION

- **Ph. D.**, Analytical Chemistry, Iowa State University, USA
- **M. S.** and **B. S.**, Chemistry, St. Stephen's College, India

PUBLICATIONS

- Dibya, D.; Sander, S.; Smith, E. A. *"Identifying cytoplasmic proteins that affect receptor clustering using Fluorescence Resonance Energy Transfer and RNA Interference"* Journal of Analytical and Bioanalytical Chemistry, 2009, 395:2303-11
- Sander, S.; Dibya, D.; Smith, E. A. *"Fluorescence-based technique for measuring intracellular cues for receptor microclustering"* submitted to J. Anal. Chimica Acta
- Dibya, D.; Arora, N.; Smith, E. A. *"Non invasive measurement of integrin microclustering under altered membrane cholesterol levels"* submitted to Biophysical Journal
- Dibya, D.; Lipert, R. J.; Porter, M. D. *"Development of Magnetic-Extrinsic Raman Labels (MERLs) for improving analysis times in SERS based immunoassays"* Manuscript in preparation
- Dibya, D.; Bergren, A. J.; Dias, N. C.; Pekas, N.; Porter, M. D. *"Rapid Pre-Screening of natural products for bioavailability by hydrophobicity and molecular weight cutoffs"* Manuscript in preparation

EXTRA CURRICULAR ACTIVITIES

- Elected Senator, Graduate Professional Student Senate (GPSS)
- Vice-president, Sankalp, Student organization at Iowa State University
- Project Coordinator, Sankalp, Student organization at Iowa State University
- Joint Secretary, Gandhi Study Circle, St. Stephen's College
- Volunteer, American Cancer Society
- Volunteer, Teacher for underprivileged students, St. Stephen's College
- Judge, Science Fair of Iowa
- Judge, Science Bowl, Ameslab, US Department of Energy

HONORS/AWARDS

- Moore Fellowship, Iowa State University 2009
- Associate Member, Sigma Xi Society 2009
- Professional Advancement Grant Award, Iowa State University 2009
- Proctor and Gamble travel award, Iowa State University 2008
- American Chemical Society travel award, Iowa State University 2008
- Outstanding Teaching Assistant, Iowa State University 2004
- Joseph F. Nelson Fellowship, Iowa State University 2003
- Need-Cum Merit Fellowship, St. Stephen's College 2002
- Freeship- Student Aid, St. Stephen's College 2001